The contribution of ocean-leaving DMS to the global atmospheric burdens of DMS, MSA, SO2, and NSS SO4=

Gondwe, M.; Krol, M.; Gieskes, W.; Klaassen, W.; de Baar, H.

Correction published 25 November 2003

The contribution of ocean-leaving DMS to the global atmospheric burdens of DMS, MSA, SO$_2$, and NSS SO$_4^=$

M. Gondwe

Marine Biology Department, University of Groningen, Haren, Netherlands

M. Krol

Institute for Marine and Atmospheric Research, University of Utrecht, Utrecht, Netherlands

W. Gieskes, W. Klaassen, and H. de Baar

Marine Biology Department, University of Groningen, Haren, Netherlands

[1]   The contribution of ocean-derived DMS to the atmospheric burdens of a variety of sulphur compounds (DMS, MSA, SO$_2$, and nss SO$_4^=$) is quantified from season to season. Such quantification, especially for nss SO$_4^=$ (the climate-relevant product of DMS oxidation), is essential for the quantification of the radiative forcing of climate that may be attributable to marine phytoplankton under possible future climate conditions. Three-dimensional chemical transport modeling up to the stratosphere is used as a tool in realizing this aim. Global data sets on oceanic and terrestrial sulphur sources are used as input. We find that the contribution of ocean-leaving DMS to the global annually averaged column burdens of the modeled compounds is considerable: 11.9 µmol m^{-2} (98% of total global burden) for DMS; 0.95 µmol m^{-2} (94% of total global burden) for MSA; 2.8 µmol m^{-2} (32% of total global burden) for SO$_2$ and 2.5 µmol m^{-2} (18% of total global burden) for nss SO$_4^=$. The mean annual contribution of DMS to the climate-relevant nss SO$_4^=$ column burden is greatest in the relatively pristine Southern Hemisphere, where it is estimated at 43%. This contribution is only 9% in the Northern Hemisphere, where anthropogenic sulphur sources are overwhelming. The marine algal-derived input of the other modeled sulphur compounds (DMS, MSA, and SO$_2$) is also greatest in the Southern Hemisphere where a lower oxidative capacity of the atmosphere, a larger sea-to-air transfer of DMS and a larger emission surface area lead to an elevation of the atmospheric DMS burden.   *INDEX TERMS:* 1615 Global Change: Biogeochemical processes (4805); 1630 Global Change: Impact phenomena; 3339 Meteorology and Atmospheric Dynamics: Ocean/atmosphere interactions (0312, 4504); 3309 Meteorology and Atmospheric Dynamics: Climatology (1620); *KEYWORDS:* global biogeochemical cycles, dimethylsulphide, sulphate aerosols, phytoplankton, climate regulation, SOLAS

1.   Introduction

[2]   Marine phytoplankton are thought to play an important role in the Earth's energy balance. Previously, a direct negative forcing of climate (i.e., a reduction in the amount of incoming solar radiation absorbed by the ocean system) was believed to be caused by an increase in the amount of solar radiation returned to the atmosphere and space through backscattering by spatially extensive and highly reflective coccolithophore blooms in the ocean [e.g., *Tyrell et al.*, 1999]. However, *Gondwe et al.* [2001] have recently found this effect to be marginal and not enough to perturb global climate.

[3]   Marine phytoplankton are further expected to make a contribution to the total radiation reflected by the Earth through indirectly adding to the atmospheric sulphate aerosol burden. Some prominent phytoplankton groups produce dimethylsulphoniopropionate (DMSP), presumably for the purpose of controlling osmotic pressure and relieving photosynthetic and oxidative stress [*Kirst*, 1996; *Stefels*, 2000; *Kiene et al.*, 2000; *Sunda et al.*, 2002]. DMSP is released into the water when microalgal cells are ruptured during consumption by zooplankton, after cell lysis at the end of a bloom or due to viral lysis [*Dacey and Wakeham*, 1986; *Malin et al.*, 1992; *Malin and Kirst*, 1997]. Dimethylsul-

---

[1]Also at Netherlands Institute for Sea Research, Texel, Netherlands.

phide (DMS) is formed as an algal or bacterial enzyme-mediated degradation product of DMSP [e.g., *Bates et al.*, 1994; *Stefels*, 2000; *Kiene et al.*, 2000]. Most of this DMS is subsequently consumed by bacteria or is photooxidized in the water [*Kiene et al.*, 2000], however, the remaining part, which forms only a small fraction of the entire in-water pool of DMS [*Kiene and Bates*, 1990]), is emitted to the atmosphere where it undergoes chemical transformation to eventually form non sea salt (nss) sulphate aerosols (SO$_4^=$) and other sulphur products [*Charlson et al.*, 1987; *Lin and Chameides*, 1993]. Sulphate aerosols play an important role in the Earth-atmosphere radiation balance through partial scattering, absorption, and reflection of solar and terrestrial radiation. They may also serve as nucleation sites for the formation of cloud droplets which, in turn, play an important role in the Earth's climate through partial scattering, reflection, and absorption of solar and terrestrial radiation.

[4] Under a possible warm future climate, it has been hypothesized that algal blooms may become more abundant and that consequently, DMS production and emissions may increase [*Charlson et al.*, 1987]. An increase in cloud condensation nuclei (as would typically result from additional sulphate aerosols of DMS origin) for a constant liquid water content, would lead to a larger concentration of cloud droplets of smaller radius, which would increase cloud optical depth [*Bates et al.*, 1987; *Charlson et al.*, 1992; *Boucher and Lohmann*, 1995; *Feichter et al.*, 1997; *Roelofs et al.*, 1998]. A decrease in mean droplet size associated with an increase in cloud droplet concentration is, furthermore, expected to inhibit precipitation development and hence increase cloud lifetime [*Feichter et al.*, 1997; *Feichter and Lohmann*, 1999]. Such an enhancement of cloud lifetime and the resultant increase in fractional cloud cover would increase both the shortwave and longwave radiative influences of clouds [*Albrecht*, 1989; *Quinn et al.*, 1995]. Inhibited precipitation development might further alter the amount and vertical distribution of water and heat in the atmosphere and thereby modify the Earth's hydrological cycle [*Charlson et al.*, 1992].

[5] Significant progress has, in the past two decades, been made to estimate the contribution of natural (biogenic (including DMS) plus volcanic) emissions of a number of sulphur compounds, to the present-day global atmospheric sulphur cycle using a variety of methods ranging from monitoring to modeling [e.g., *Schwartz*, 1988; *Langner and Rodhe*, 1991; *Ayers et al.*, 1991; *Bates et al.*, 1992a; *Benkovitz et al.*, 1994; *Prospero et al.*, 1995; *Chin et al.*, 1996, 2000a, 2000b; *Chin and Jacob*, 1996; *Pham et al.*, 1996; *Feichter et al.*, 1996, 1997; *Bates and Quinn*, 1997; *O'Dowd et al.*, 1997; *Roelofs et al.*, 1998; *Davis et al.*, 1998; *Koch et al.*, 1999; *Chen et al.*, 2000; *Barth et al.*, 2000; *Rasch et al.*, 2000]. With regard to monitoring, some ice core and atmospheric measurement studies [e.g., *Legrand et al.*, 1991, 1997; *Li et al.*, 1993a; *Berresheim et al.*, 1990, 1991, 1998; *Saltzman et al.*, 1983, 1985; *Ayers et al.*, 1991; *Savoie et al.*, 1989, 1992, 1993, 1994; *Prospero et al.*, 1991, 1995; *Mulvaney et al.*, 1992] have used the MSA: nss SO$_4^=$ ratio (MSA = methanesulphonate) to estimate the biogenic fraction of SO$_4^=$ over various areas. MSA is formed exclusively from DMS while nss SO$_4^=$ has a

variety of sources which include DMS oxidation and volcanic and industrial sulphur emissions, and so this ratio provides a rough indication of the relative contributions of biogenic and anthropogenic sources to total sulphate levels. However, since such measurements are localized, they have the deficiency of not being spatially comprehensive. The contribution of oceanic DMS to the total sulphur cycle relative to an anthropogenic source can be expected to differ in different areas of the globe and at different times of the year depending on the location and strength of major anthropogenic sulphur sources and the atmospheric conditions prevailing in different regions and at different times of the year. Thus, while MSA: nss SO$_4^=$ ratio studies provide useful insights on the relative biogenic contribution to the sulphur cycle in specific locations, three-dimensional global studies are more appropriate for providing a globe-wide picture of the spatial variation and distribution of this ratio and can help in excluding the possibility that the significance attached to the relationships proposed by the ratio in one area are not completely different elsewhere or at another time of the year.

[6] With respect to modeling studies, most [e.g., *Langner and Rodhe*, 1991; *Benkovitz et al.*, 1994; *Pham et al.*, 1996; *Feichter et al.*, 1996; *Chin and Jacob*, 1996; *Koch et al.*, 1999; *Chin et al.*, 2000a, 2000b; *Boucher and Pham*, 2002] have focused on apportioning burdens of DMS and/or MSA and/or SO$_2$ (sulphur dioxide) and/or SO$_4^=$ to either natural (volcanic plus biogenic) or anthropogenic sources. In the current study, we focus on isolating and quantifying the fraction of the atmospheric burdens of all four compounds which can be attributed to oceanic algae alone versus those which can be attributed to all other sources (anthropogenic plus all other natural sources). As long as this individual contribution remains unknown, or hidden within the numbers quantifying the total biogenic fraction, quantifying and judging the significance of the climatic effects induced by marine algae alone remains difficult.

[7] Within these modeling studies, *Benkovitz et al.* [1994] report on sulphate column burdens, but only above the North Atlantic Ocean for selected days in 2 months. *Benkovitz et al.* [1994], *Feichter et al.* [1996], *Chin and Jacob* [1996], *Kasibhatla et al.* [1997] and *Koch et al.* [1999] present results on the troposphere only. However, it is now being strongly recognized that the inclusion of the stratosphere in global 3-D chemical transport modeling is desirable, especially if radiatively active tracers such as ozone and water vapor are included [e.g., *Steil et al.*, 1998]. Changes in such tracers feedback on dynamic processes within the troposphere and stratosphere which in turn feedback on the spatial distribution of chemical species within the model. *Barth et al.* [2000] and *Rasch et al.* [2000] omit volcanic and biomass burning sources from their simulations. Since these are significant contributors to the total sulphur cycle, their omission can result in a bias in the simulated percentage contributions from considered sources. *Langner and Rodhe* [1991] and *Feichter et al.* [1996] consider SO$_2$ as the sole product of DMS oxidation while *Langner and Rodhe* [1991] and *Benkovitz et al.* [1994] consider the hydroxyl radical (OH) as the sole oxidant of DMS. Today, MSA is also a known DMS oxidation product

and the gaseous nitrate radical (NO_3) is recognized as an additional DMS oxidant. *Raes et al.* [2000] report the relative importance of DMS oxidation to total SO_2 concentrations at selected levels of the troposphere.

[8] Through use of a comprehensive global 3-D chemical transport modeling study for 19 vertically stacked layers, with five layers in the planetary boundary layer ($\sim$1000–810 hPa), nine in the free troposphere (810–120 hPa), and five in the stratosphere (120–1 hPa), we build upon the results of the above studies. Oceanic DMS emissions are calculated from a globally interpolated sea surface DMS database [*Kettle et al.*, 1999] and we use the *Andres and Kasgnoc* [1998] database on volcanic emissions which supercedes that used in most other modeling studies discussed above. We report here on the atmospheric column burdens of DMS, MSA, SO_2, and nss SO_4^- resulting from both oceanic and terrestrial sources and those resulting from oceanic DMS emissions alone. Such quantification of the present-day global column burdens, especially for nss SO_4^-, is important for the further quantification of the radiative forcing of climate attributable to aerosols of oceanic algal origin under predicted future meteorological conditions.

2. Data and Methodology

[9] We make use of version 3 of the 3-D global Chemical Transport Model (Tracer Model 3; TM3) [*Houweling et al.*, 1998; *Dentener et al.*, 1999, 2002; *Jeuken et al.*, 2001]. The model contains comprehensive sulphur chemistry schemes treating the emission of sulphur species from various source types and the removal of sulphur species through both physical processes (dry and wet deposition) and chemical transformation (photochemical, heterogeneous, gas phase, and aqueous phase reactions) [*Jeuken et al.*, 2001]. The distribution of chemical species is controlled by 6-hour mean large-scale dynamics defined by ECMWF (European Centre for Medium Range Weather Forecasts) analyses. Computations are made hourly for the meteorologically representative year of 1993. However, we analyze and present results on monthly averaged fields since our focus is on climatology. The model was spun up by first running it for a couple of months (November and December). Initialization of 1 November was executed with the October monthly mean values of a 1-year run. Output was collected for the entire year of 1993 from 1 January to 31 December. The input data used in this study are aggregated from their original resolutions to the working resolution of $7.5° \times 10°$ and for 19 vertically stacked layers (up to the stratosphere). It is also possible to run TM3 at finer resolutions [e.g., see *Jeuken et al.*, 1999, 2001; *Dentener et al.*, 1999, 2002].

[10] Both terrestrial and oceanic sources of sulphur have been considered. Anthropogenic sources in continental areas include SO_2 producing industrial activities and biomass burning. TM3 inputs on these have been obtained from the Emission Database for Global Atmospheric Research (EDGAR database) [*Olivier and Berdowski*, 2001]. Terrestrial biogenic sulphur emissions include those of DMS from plants, soils, wetlands, and freshwater lakes. TM3 inputs on these have been based on work by *Spiro et al.* [1992] (0.9 Tg S yr^{-1}). Oceanic DMS emissions (18 Tg S yr^{-1}) are calculated based on globally interpolated sea surface DMS concentrations obtained from the *Kettle et al.* [1999] database which is currently held and distributed by the University Corporation for Atmospheric Research (UCAR) (available at http://dss.ucar.edu/datasets/ds289.2/). For the calculation of these emissions, we make use of surface winds within TM3 and the *Liss and Merlivat* [1986] air-sea exchange model, which predicts the flux of gases across the air-sea interface as being proportional to the product of the concentration difference across the sea-air interface and the gas transfer velocity. This method is widely used and has previously been well described in literature [e.g., *Andreae*, 1986; *Charlson et al.*, 1987; *Bates et al.*, 1992b, 1994; *Malin et al.*, 1992; *Chin et al.*, 1996; *Davison et al.*, 1996; *Gabric et al.*, 1996, 1998; *Frost and Upstill-Goddard*, 1999].

[11] Recently, sulphur emissions from fossil fuel burning by international shipping have been found to be a significant contributor to atmospheric SO_2 concentrations over most of the global ocean [*Capaldo et al.*, 1999; *Corbett et al.*, 1999]. We include ship emissions in our analyses and utilize emission data from the EDGAR database. The total anthropogenic SO_2 emission considered from the EDGAR database is 78 Tg S yr^{-1}. SO_2 released from volcanoes (13.4 Tg yr^{-1}) is based upon a 25-year global measurement record which has been compiled into a GEIA (Global Emissions Inventory Activity) database by *Andres and Kasgnoc* [1998]. Both sporadically and continuously erupting volcanoes are considered in this database. In their database, Andres and Kasgnoc assume that sporadic fluxes last only one day and, therefore, sum up the measured SO_2 fluxes from continuously and sporadically emitting volcanoes to produce a combined flux in mass per day. However, on an annual basis, Andres and Kasgnoc note that sporadically emitting volcanoes account for <1% of the total summed flux. Furthermore, each volcano has a unique injection altitude. The injection altitude of the volcanoes included in the inventory varies between 321 and 5592 m. In our model, the volcanoes are considered as point sources, which means that their emissions are localized and not interpolated over the entire globe.

[12] Figure 1 shows a simplified schematic representation of the DMS oxidation process as considered by TM3. In the vertical dimension, DMS loss in TM3 mainly occurs in the boundary layer, followed by the free troposphere (Table 1). The polar stratosphere plays a negligible role in DMS chemistry while DMS chemistry is slightly more important in the tropical stratosphere where large scale convective transport inputs DMS into the stratosphere.

[13] The destruction of DMS occurs in the gas phase and is characterized by its daytime oxidation by OH and its nighttime reaction with NO_3 [*Atkinson et al.*, 1984; *Kreidenweis et al.*, 1991; *Hynes et al.*, 1993; *Atkinson et al.*, 1997], with these reactions being most effective in the tropical and subtropical zones (see Table 1). In general, field measurements and laboratory experiments indicate that MSA and SO_2 are the dominant stable products formed from these reactions. TM3 considers two major DMS reaction pathways for the formation of SO_2 and MSA [*Hynes et al.*, 1986, 1993; *Atkinson et al.*, 1992; *Koga and Tanaka*, 1993]: one where
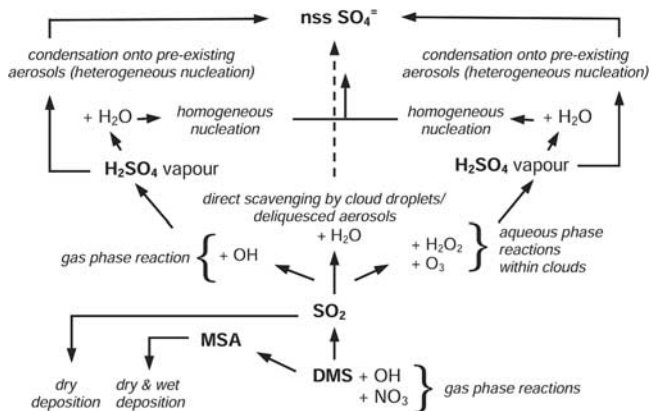
Figure 1. A simplified schematic representation of DMS loss and sulphate aerosol formation processes as considered by the TM3 model.

both OH and NO_3 abstract a hydrogen atom from a DMS molecule leading to the formation of several intermediate products and eventually SO_2 as a stable end-product and one where OH is added to the S-atom in DMS to eventually yield 25% MSA and 75% SO_2 [*Hynes et al.*, 1986] as stable end-products. The second reaction pathway is effective under low ambient temperatures [*Hynes et al.*, 1986; *Barone et al.*, 1995; *Arsene et al.*, 2001]. The rate coefficient (cm^3 molecules^{-1} s^{-1}) and its temperature dependence function as used in TM3 for DMS + OH $\rightarrow$ SO_2 + ... is 9.6×10^{-12} exp($-234/T$) following *Hynes et al.* [1986] and *Atkinson et*

al. [1992]. That for DMS + OH $\rightarrow$ 0.75 SO_2 + 0.25 MSA is $k_1M/(1. + k_2M)$, where $k_1 = 1.7 \times 10^{-42}$ exp(7810./T), $k_2 = 5.5 \times 10^{-31}$ exp(7460./T) and $M = O_2$ (molecules cm^{-3}) following *Hynes et al.* [1986]. The rate coefficient and its temperature dependence function for DMS + NO_3 $\rightarrow$ SO_2 + ... as used in TM3 is 1.9×10^{-13} exp (520/T) following *Atkinson et al.* [1992].

[14] MSA is removed from the atmosphere through wet and/or dry deposition while SO_2 loss occurs through dry deposition and both gas and aqueous phase reactions. In the gas phase, SO_2 is oxidized by OH to form sulphuric acid (H_2SO_4) while in the aqueous phase (within clouds), it is oxidized by hydrogen peroxide (H_2O_2) and ozone (O_3), when present, also to form H_2SO_4 [*Penkett et al.*, 1979; *Ghan et al.*, 1989; *Crutzen and Zimmermann*, 1991; *Langner and Rodhe*, 1991; *Lin and Chameides*, 1993; *Benkovitz et al.*, 1994; *Chin et al.*, 1996; *Lelieveld et al.*, 1997; *Feichter et al.*, 1997; *Roelofs et al.*, 1998]. The H_2SO_4 formed from SO_2 oxidation undergoes bimolecular homogeneous nucleation with water vapor to form new sulphate aerosols or it condenses onto pre-existing aerosols (heterogeneous nucleation) [e.g., *Kreidenweis and Seinfeld*, 1988; *Kreidenweis et al.*, 1991]. These physical processes increase the number and size of the sulphate particles, respectively. All chemistry in TM3 is calculated on-line, which means that the oxidant fields (OH, NO_3, H_2O_2 and O_3) contain the variability from both transport and the diurnal cycle. An analysis of the sulphur budget in TM3 and the relative importance of DMS oxidation pathways in the model atmosphere per geographical region has been made and is presented in Table 1.

Table 1. Annual Sulphur Budget in TM3: Relative Importance of DMS Oxidation Pathways in the Model Atmosphere per Geographical Region[a]

	Contribution and Relative Importance by Region, Megamole S yr^{-1}			
	90°N–45°N	45°N–Eq	Eq–45°S	45°S–90°S
DMS emissions	50933 (100:0:0)	172917 (100:0:0)	238673 (100:0:0)	129937 (100:0:0)
Initial atmospheric DMS burden	1484 (33:66+:<1)	760 (61:38+:<1)	978 (85:14+:<1)	1987 (80:19+:<1)
DMS loss by 'DMS + OH $\rightarrow$ SO_2'	−10292 (78:21+:<1)	−65597 (81:18+:<1)	−116736 (78:21+:<1)	−36329 (66:33+:<1)
DMS loss by 'DMS + OH $\rightarrow$ 25% MSA + 75% SO_2'	−16517 (68:31+:<1)	−48923 (62:36:2)	−99599 (63:36:1)	−72014 (57:42+:<1)
DMS loss by 'DMS + NO_3 $\rightarrow$ SO_2'	−24993 (73:26+:<1)	−63466 (83:16+:<1)	−33821 (69:30+:<1)	−4095 (52:46:2)
Final DMS burden	1492 (33:66+:<1)	766 (60:39:1)	989 (85:14+:<1)	2042 (80:19+:<1)
Initial MSA burden	15 (23:51:26)	99 (26:61:13)	294 (46:50:4)	340 (59:40:1)
MSA production from DMS + OH $\rightarrow$ 25% MSA	4129 (68:31+:<1)	12231 (62:36:2)	24900 (63:36:1)	18004 (57:42+:<1)
MSA loss by dry deposition	−534 (100:0:0)	−1341 (100:0:0)	−3167 (100:0:0)	−2687 (100:0:0)
MSA loss by wet deposition	−3753 (58:41+:<1)	−11440 (64:34:2)	−21016 (67:32:1)	−15323 (51:48+:<1)
Final MSA burden	15 (23:50:27)	99 (26:61:13)	296 (46:50:4)	341 (58:40:2)
SO_2 emissions	597835 (99+:<1:0)	1742849 (93:7:0)	316533 (76:24:0)	1185 (27:73:0)
Initial SO_2 burden	20728 (43:56+:<1)	10748 (67:32:1)	746 (40:50:10)	352 (46:51:3)
SO_2 production from DMS + OH $\rightarrow$ SO_2	10292 (78:21+:<1)	65597 (81:18+:<1)	116736 (78:21+:<1)	36329 (66:33+:<1)
SO_2 production from DMS + OH $\rightarrow$ 75% SO_2	12388 (68:31+:<1)	36692 (62:36:2)	74699 (63:36:1)	54010 (57:42+:<1)
SO_2 production from DMS + NO_3 $\rightarrow$ SO_2	24993 (73:26+:<1)	63466 (83:16+:<1)	33821 (69:30+:<1)	4095 (52:46:2)
SO_2 loss by dry deposition	−339742 (100:0:0)	−739115 (100:0:0)	−82180 (100:0:0)	−8106 (100:0:0)
SO_2 loss by wet deposition	−125053 (70:29+:<1)	−569473 (77:22+:<1)	−241909 (76:23+:<1)	−53995 (60:39+:<1)
SO_2 loss by SO_2 + OH $\rightarrow$ $SO_4^=$	−40174 (81:18+:<1)	−157161 (77:22:1)	−27850 (60:38:2)	−1705 (41:56:3)
SO_2 loss by SO_2 + O_3 $\rightarrow$ $SO_4^=$	−9385 (56:44:0)	−56324 (38:62:0)	−45707 (41:59:0)	−5162 (65:35:0)
SO_2 loss by SO_2 + H_2O_2 $\rightarrow$ $SO_4^=$	−102204 (54:46:0)	−419147 (60:40:0)	−141402 (62:38:0)	−25706 (63:37:0)
SO_2 final concentration	20749 (43:56+:<1)	10714 (67:32:1)	746 (40:50:10)	349 (45:52:3)

[a]Values in parentheses are the percentage contribution in the boundary layer (model layers 1–5; ~1000–810 hPa): percentage contribution in the free troposphere (model layers 6–14; 810–120 hPa): percentage contribution in the stratosphere (model layers 15–19; 120–1 hPa). The values presented here are for a closed budget. Overestimation of DMS and SO_2 loss by TM3 is small (0.003% and 0.1%, respectively).

[15] TM3 makes use of a technique (referred to as tagged or colored tracers) to label molecules of DMS originating from an oceanic source and subsequently the molecules of MSA, SO$_2$, and nss SO$_4^=$ produced from it. This has made the model specifically suitable for realizing the aim of this study, i.e., isolating the fraction of the total atmospheric burdens of DMS, MSA, SO$_2$, and nss SO$_4^=$ that can be attributed to oceanic-algal derived DMS emissions.

[16] Extensive validation of the TM3 model for modeling the relative yields of SO$_2$ and sulphate in the global atmospheric sulphur cycle, under a setup similar to ours and for the same model year, has previously been made by *Jeuken et al.* [2001] and will not be repeated here. Model performance was generally found to be satisfactory. However, some shortcomings were noticed in winter when SO$_4^=$ was slightly underestimated and SO$_2$ was overestimated due to shortcomings in the winter SO$_2$ oxidation processes in the model. Validation of DMS and MSA outputs was not made by *Jeuken et al.* [2001] and so we analyze TM3 results against published marine boundary layer measurements of these species where available (Table 2). Discussion of Table 2 occurs within various appropriate paragraphs of section 3.

3. Results and Discussion

3.1. Dimethylsulphide (DMS)

[17] December–January–February, June–July August and annual mean column burdens of atmospheric DMS resulting from both oceanic and terrestrial sources (hereafter referred to as "all" sources) are shown in plot a1 in Figures 2, 3, and 4, respectively. The highest burdens (even during June–July August, the Northern Hemispheric summer) occur in the Southern Hemisphere, specifically in a broad band above the Southern Ocean (also see plot a1 in Figures 5 and 6). This is, at first glance, surprising, as the highest seawater DMS concentrations occur in the hemisphere that is experiencing summer and where phytoplankton occurrence and seawater DMS concentrations are also highest [*Kettle et al.*, 1999]. However, this effect may partly be explained through the different atmospheric oxidative capacities of the two hemispheres. The lifetime of DMS depends upon the atmospheric concentration of its two major oxidants: OH and NO$_3$, both of which are NO$_x$ (nitrogen oxides = NO (nitrous oxide) + NO$_2$ (nitrogen dioxide)) dependent [*Crutzen and Zimmermann*, 1991; *Thompson et al.*, 1993; *Davison et al.*, 1996; *Andreae and Crutzen*, 1997].

[18] OH is formed primarily as a result of photolysis of O$_3$ by solar ultraviolet radiation and the subsequent reaction of the photolysis product O(^{1}D) with water vapor [*Crutzen and Zimmermann*, 1991]. Tropospheric O$_3$ is in turn produced by the photochemical oxidation of NO$_x$ and hydrocarbons, both of which have strong anthropogenic sources. The reaction of OH with many species also initiates a catalytic cycle which reforms OH. For example, the reaction of OH with carbon monoxide (CO) in the presence of oxygen produces hydroperoxyl radicals (HO$_2$) and carbon dioxide (CO$_2$). In turn, the HO$_2$ which is formed reacts with NO to reform OH and also produce NO$_2$. This NO$_2$ may in turn be photolyzed in the presence of oxygen to form NO and O$_3$.

O$_3$ is further photolyzed, and in the presence of water vapor reforms OH.

[19] Although the oxidant formation mechanisms operate in the same way all over the globe, the larger and more industrialized landmasses of the Northern Hemisphere ensure an ample supply of OH and NO$_3$ to the Northern Hemispheric atmosphere, and therefore greater DMS removal. Even during the dark winter months around the North Pole, industrial emissions from the nearby continents ensure an abundant supply of NO$_3$ (verified by long-term measurements of aerosol nitrate (NO$_3^-$) from a network of stations [*Prospero et al.*, 1995]), which continues to oxidize DMS in the absence of OH. OH production and abundance are sunlight driven and so OH exists only during daytime and is not available as an oxidant for the removal of DMS in the dark winter months at high latitudes. NO$_3$, on the other hand, has a nighttime abundance and a daytime scarcity due to its rapid photolysis [*Atkinson*, 1991; *Wayne et al.*, 1991] and so is the major oxidant of DMS during dark periods. The less industrialized Southern Hemisphere (especially the remote area south of 50°S) has a limited supply of NO$_3$ for the removal of DMS during the long dark winter months of June–July August (also verified by long-term measurements of aerosol nitrate on Antarctica [*Savoie et al.*, 1993]), resulting in an accumulation of DMS and an increase in its atmospheric burden.

[20] Measurements of both seawater and atmospheric concentrations of DMS during a ship cruise along a transect through the Atlantic Ocean by *Burgermeister et al.* [1990] led to the same conclusion. Although seawater DMS concentrations were measured to be higher in the North Atlantic than in the South Atlantic, these authors found that the mean atmospheric DMS concentration was higher above the South Atlantic than above the North Atlantic. They attributed this to a faster oxidation of DMS in the Northern Hemisphere.

[21] Our findings of a high DMS burden above Antarctica throughout the year are also supported by field/model studies by *Davis et al.* [1998] during Project SCATE in the austral summer. These authors observed a very shallow marine boundary above the Palmer peninsula in which UV levels (and, therefore, OH production) are reduced. The consequently diminished oxidative removal of DMS resulted in an extended DMS lifetime of 7–9 days, which is relatively high for the summer period (elsewhere, the lifetime of DMS has been estimated to vary from approximately half a day in summer to about a week in winter [*Gabric et al.*, 1996]). If DMS was found to have such a long lifetime in summer when OH levels are at their highest, one can presume at least a similar, if not longer, lifetime of DMS above Antarctica during the long dark winter months when OH is absent and NO$_3$ is minimal.

[22] Next to atmospheric chemistry, atmospheric dynamics and orography also play an important role in determining the magnitude of the DMS burden in a particular location within a hemisphere. In the Northern Hemisphere, a larger land surface area and orography perturb the atmospheric circulation encouraging the mixing of air masses and their chemical contents between the low, middle, and high latitudes. This leads to the spatial dilution of DMS concen-

Table 2. Observed Versus Modeled Boundary Layer Concentrations of DMS and MSA Resulting From All Sources

Site	Period	Surface Concentration,[a] ppt				Reference[b]
		DMS		MSA		
		Observed	Modeled	Observed	Modeled	
Arctic						
Alert, Canada	'80–'91	–	–	1.8	3.5	LI1, LI2, LB
Barrow, Alaska	Feb–Apr '88	–	–	0.4–1.7	1.5	LI1
	Mar–Apr '89	–	–	1.5	1.8	LI1
Dye, Greenland	Aug '88–Jul '89	–	–	0.35	3.0	LI1
Summit, Greenland	Jun–Jul '89	–	–	0.7	7.5	LI1
	Jun–Aug '90	–	–	1.4	8	LI1
North and South Atlantic						
N. Atlantic (open ocean)	Apr–May '84	75	80	–	–	AN1
Along U.S. East Coast	Sep '85–Sep '86	683	30	–	–	BE3
Off U.S. East Coast	Sep '85–Sep '86	33.3	20	–	–	BE3
	Aug–Sep '89	<DL-150	20	–	–	JB, CS, AN2, GR
Off and along U.S. East Coast	Sep '85–Sep '86	–	–	7.9	1.3	BE3
Sargasso Sea	Jun '84	178	40	–	–	AN1
Gulf of Mexico	Oct '85	25	20	–	–	SC
Miami	Jul '91–Mar '93	–	–	10.3	1.5	PR
Tropical S. Atlantic	Aug–Sep '89	9–104	70	–	–	JB, CS, AN2, GR
	Feb–Mar '91	50–300	50	–	–	AN3, AN4, SU
Bahamas	Nov '83	94	140	–	–	AN1
	Jun '85	154	80	–	–	SC
Barbados	Jul '91–Mar '93	–	–	4.7	1.9	PR
Bermuda	Jul '91–Mar '93	–	–	8.5	1.9	PR
Caribbean Transect	Feb–Mar '86	83	50	–	–	SC
Heimaey, Iceland	Jul '91–Mar '93	–	–	8.7	4.1	PR
Mace Head, Ireland	Jul '91–Mar '93	–	–	13.6	4.8	PR
United Kingdom	1988–1990	45	109	1.41	4.8	DH
Tenerife	Jul '91–Mar '93	–	–	0.94	2.5	PR
Eastern Mediterranean (Greece)	May '97–Oct '99	55	25	–	–	KM
	Oct '96–Sep '99	–	–	6.3	1.5	KM
Atlantic Ocean Transects						
S. Atlantic	Mar–Apr '87	23.5	50	–	–	BU
N. Atlantic	Mar–Apr '87	20	40	–	–	BU
Iceland to Argentina (60°N–45°S)	Oct '96	29–396	1–240	–	–	SR
U.K. to Antarctica	Oct '92–Jan '93	<DL – 549	1–400	0.4–85	1–48	DV
Southern Ocean + Antarctic						
Drake Passage, Bransfield and Gerlache Straits	Mar–Apr '86	96	410	6.2	10.6	BE1
Drake Passage	Nov–Dec '90	147	390	–	–	SG
Weddell Sea	Nov–Dec '90	23	340	–	SG	
S. Atlantic (68°S, 4°W)	Nov–Dec '90	671	510	–	SG	
Palmer	Apr '90–May '91	–	–	11.5	15.7	SA3
	Jan–Feb '94	6–595	85	3.3–146	55	BE4
Mawson	Mar '87–Dec '91	–	–	5.4	10.3	SA2, SA3
	Jul '91–Mar '93	–	–	4.9	10.3	PR
Marsh	Apr '90–Apr '91	–	–	7.1	12.7	SA3
Cape Grim	Jan–Feb '84	128	25	–	–	AN1
	Nov '88–May '96	12–235	10–140	0.47–50	2–30	AY1, GI, AG
	Nov '88–Mar '93	55	64	–	–	AY3
	'76–'91	–	–	4.1	10.6	AY2, GI
Southern Ocean, off Cape Grim	Dec '86	15–60	80	11	16	BE2
	Nov–Dec '95	24–350	80	–	–	BR
Macquarie Island	Dec '88–Sep '91	–	–	<0.2–16.5	9	GI
North Pacific						
Midway Island	'81–'87	–	–	7.1	5	SA1
	'81–'82	–	–	7.1	5	SP
Shemya Island	'81–'86	–	–	22.8	7.2	SP, SA1
Equatorial Pacific						
	Feb–Mar '91	352	200	10	5	HU
	July '82	124	290	–	–	AN1
	'81–'86	–	–	10.3	4.8	SA1
Fanning Island	Apr '81–Aug '82	–	–	10.6	4.8	SZ, SP

Table 2. (continued)

Site	Period	Surface Concentration,[a] ppt				Reference[b]
		DMS		MSA		
		Observed	Modeled	Observed	Modeled	
South Pacific						
American Samoa						
	Mar '83 – Aug '84	–	–	6.1	3.4	SZ, SP
	03/83 – 04/84, 01/90 – 04/92	–	–	5.4	3.4	SA4
	Jul '91 – Mar '93	–	–	5.9	3.4	PR
Norfolk Island	'83 – '87	–	–	5.6	3.4	SA1
	'83 – '87	–	–	5.4	6.3	SA1
New Caledonia	'83 – '84	–	–	5.9	6.3	SP
	'83 – '87	–	–	4.7	4.2	SA1
Leigh, New Zealand	'83 – '84	–	–	5.9	4.2	SP
	Dec '90 – Nov '92	5.9 – 350	50 – 150	–	–	WM
	1991, 1992	–	–	11.5, 19	8.4	WM
Indian Ocean						
Amsterdam Island	'84, '87, '88, '89	23.5 – 376	30 – 300	–	–	NG

[a]Where a range is given the values correspond to a minimum and maximum. A single value represents a mean. <DL means below detection limit.
[b]AG: *Ayers and Gillet* [2000]; AN1: *Andreae et al.* [1985]; AN2: *Andreae et al.* [1993]; AN3: *Andreae et al.* [1994]; AN4: *Andreae et al.* [1995]; AY1: *Ayers et al.* [1991]; AY2: *Ayers et al.* [1986]; BE1: *Berresheim* [1987]; BE2: *Berresheim et al.* [1990]; BE3: *Berresheim et al.* [1991]; BE4: *Berresheim et al.* [1998]; BR: *De Bruyn et al.* [1998]; BU: *Burgermeister et al.* [1990]; CS: *Cooper and Saltzman* [1993]; DH: *Davison and Hewitt* [1992]; DV: *Davison et al.* [1996]; GI: *Gillett et al.* [1993]; GR: *Gregory et al.* [1993]; HU: *Huebert et al.* [1993]; JB: *Johnson and Bates* [1993]; KM: *Kouvarakis and Mihalopoulos* [2002]; LB: *Li and Barrie* [1993]; LI1: *Li et al.* [1993a]; LI2: *Li et al.* [1993b]; NG: *Nguyen et al.* [1992]; PR: *Prospero et al.* [1995]; SA1: *Savoie et al.* [1989]; SA2: *Savoie et al.* [1992]; SA3: *Savoie et al.* [1993]; SA4: *Savoie et al.* [1994]; SC: *Saltzman and Cooper* [1988]; SG: *Staubes and Georgii* [1993]; SP: *Savoie and Prospero* [1989]; SR: *Sciare et al.* [2000]; SU: *Suhre et al.* [1995]; SZ: *Saltzman et al.* [1985]; WM: *Wylie and de Mora* [1996].

trations. On the other hand, the Southern Hemisphere has a greater oceanic surface area, with most of the landmasses being concentrated in the low latitudes. Atmospheric perturbation and consequent meridional mixing between the low and middle and high latitudes is, therefore, limited. The strongly zonal southern circumpolar flow results in the local elevation of the DMS burden in the middle and high latitudes.

[23] In addition to differing oxidative capacities and orography, the Southern Hemisphere has a greater ocean surface area from which DMS is emitted when compared to the Northern Hemisphere. Furthermore, the sea-to-air transfer of gases has generally been found to be higher in rough and stormy seas [e.g., *Watson et al.*, 1991]. Frequent and rough storms which track along the high southern latitudes result in higher concentrations of DMS in the Southern Hemispheric atmosphere than in the Northern Hemispheric atmosphere. *Burgermeister et al.* [1990] measured relatively low atmospheric DMS concentrations over the North Atlantic, where the mean DMS supersaturation in the water was a factor of 6 higher than that determined in the South Atlantic on the same measurement campaign. They similarly attributed this to a diminished gas exchange between water and air, which could have been caused by the lower mean wind speeds simultaneously measured in the North Atlantic. High atmospheric DMS concentrations measured in the English Channel toward the end of the cruise by these authors were partly attributed to increased fog and subsequent decreased incident solar radiation which reduced the photochemical production of OH, a major DMS oxidant.

[24] Comparisons of globally observed and modeled boundary layer concentrations are made in Table 2. The relatively coarse spatial resolution which we have selected for our model runs inhibits exact point-to-point correlation

of the magnitude of modeled results with measurements. Nevertheless, the values are presented and comparisons in spatial and temporal trends are made. TM3 performs reasonably well in simulating atmospheric DMS concentrations over most regions, but overestimates concentrations above the Drake Passage and Weddell Sea off Antarctica as well as above the United Kingdom. Some underestimation is noted in the Eastern Mediterranean and Sargasso Sea. These differences may be attributed to differences in the temporal scales of the measurements and the modeled concentrations. Most of the observed data are multiyear measurements (spanning even up to 11 years for MSA). The effects of meteorology (e.g., changes in wind speed and source direction) on concentrations recorded at a monitoring station and the location of hot spots are, therefore, smoothed out in these measurements. Our modeled concentrations are based on a 1-year record, which is inevitably strongly influenced by the specific meteorology of that year. Temporal trends are, in general, reasonably well reproduced by the model, with concentrations being higher in summer than in winter (e.g., at Cape Grim [*Ayers and Gillett*, 2000]). Global spatial patterns of lower atmospheric DMS (and MSA) reproduced by TM3 are comparable to those modeled by *Chin et al.* [1996, 2000a] and *Koch et al.* [1999].

[25] The global spatial distribution and magnitude of December – January – February, June – July August and annually averaged column burdens of atmospheric DMS of oceanic origin (plot a2 in Figures 2, 3, and 4, respectively) are largely similar to those of DMS resulting from all sources (also see plot a1 versus plot a2 in Figures 5 and 6). The contribution of seawater DMS to the column burden of atmospheric DMS within the tropics is low relative to that in extratropical regions (Figures 5 (plot a3) and 6 (plot a2)).
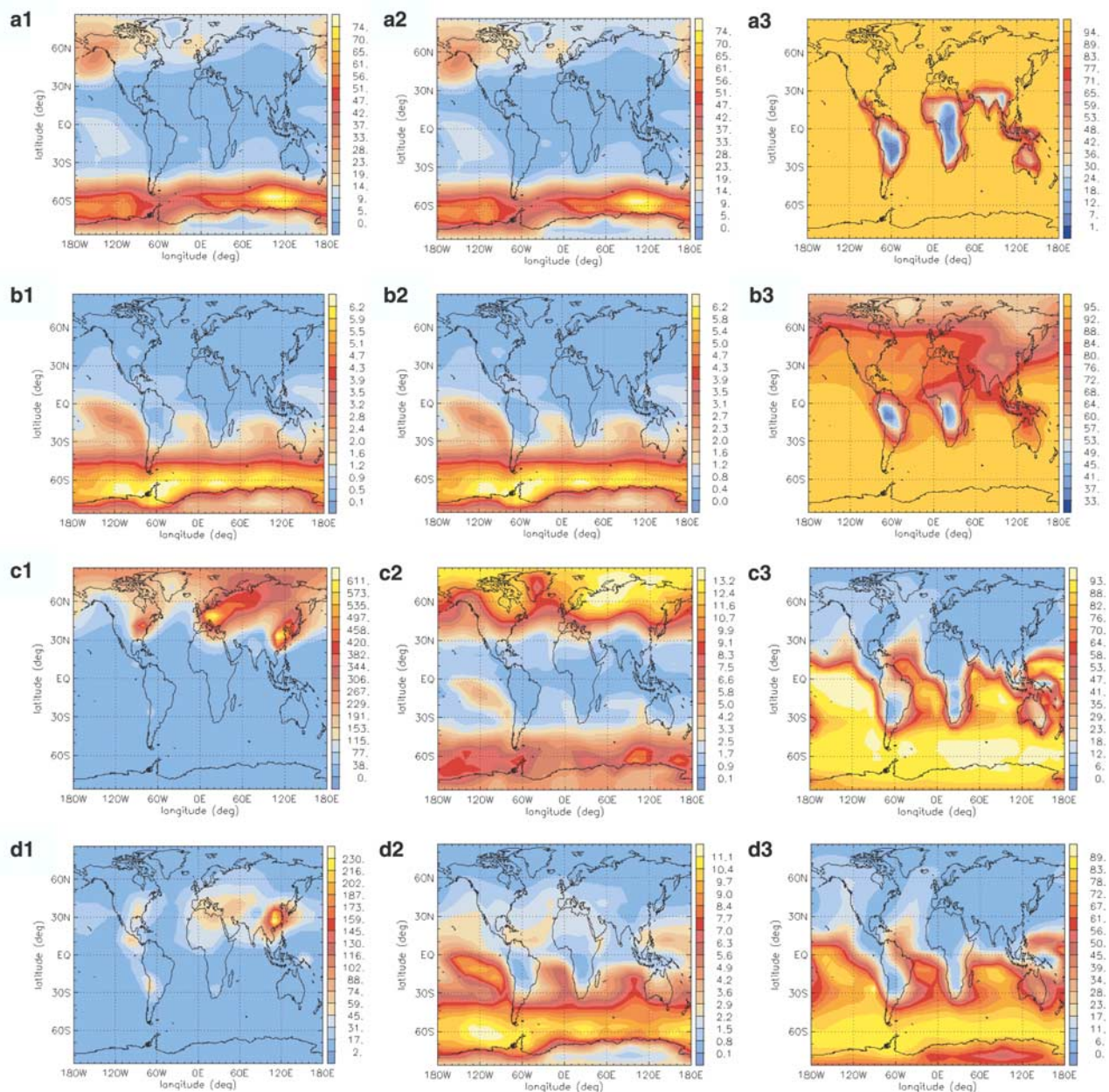
Figure 2. (a1, b1, c1, d1) December–January–February mean column burdens (μmol m^{-2}) of DMS, MSA, SO$_2$ and nss SO$_4^=$, respectively, resulting from both oceanic and terrestrial sources; (a2, b2, c2, d2) those resulting from oceanic DMS emissions alone; and (a3, b3, c3, d3) the percentage of December–January–February averaged column burdens of DMS, MSA, SO$_2$ and nss SO$_4^=$, respectively, that can be attributed to oceanic DMS emissions alone.

This is due to the fact that terrestrial DMS emissions are highest in the warm and wet tropical areas, where they have a very small seasonal cycle, and where they overwhelm the oceanic source.

[26] The globally averaged annual mean burden of DMS of oceanic origin is 11.9 μmol m^{-2} (98% of the total global DMS burden, Table 3). This huge contribution is not surprising since oceanic DMS emissions are globally the largest atmospheric DMS source. Spatially, the contribution of seawater DMS to the total column burden of DMS is

greatest over all oceanic and polar regions in all seasons (plot a3 in Figures 2, 3, and 4). The lowest contribution occurs above continental regions, where terrestrial sources are more important and where oxidant levels are higher. The flux of DMS from continental sources increases exponentially with temperature [*Bates et al.*, 1992a]. This temperature dependence results in a significant seasonal cycle of atmospheric DMS burdens at continental high latitudes, but not within the tropics where temperatures are more stable.
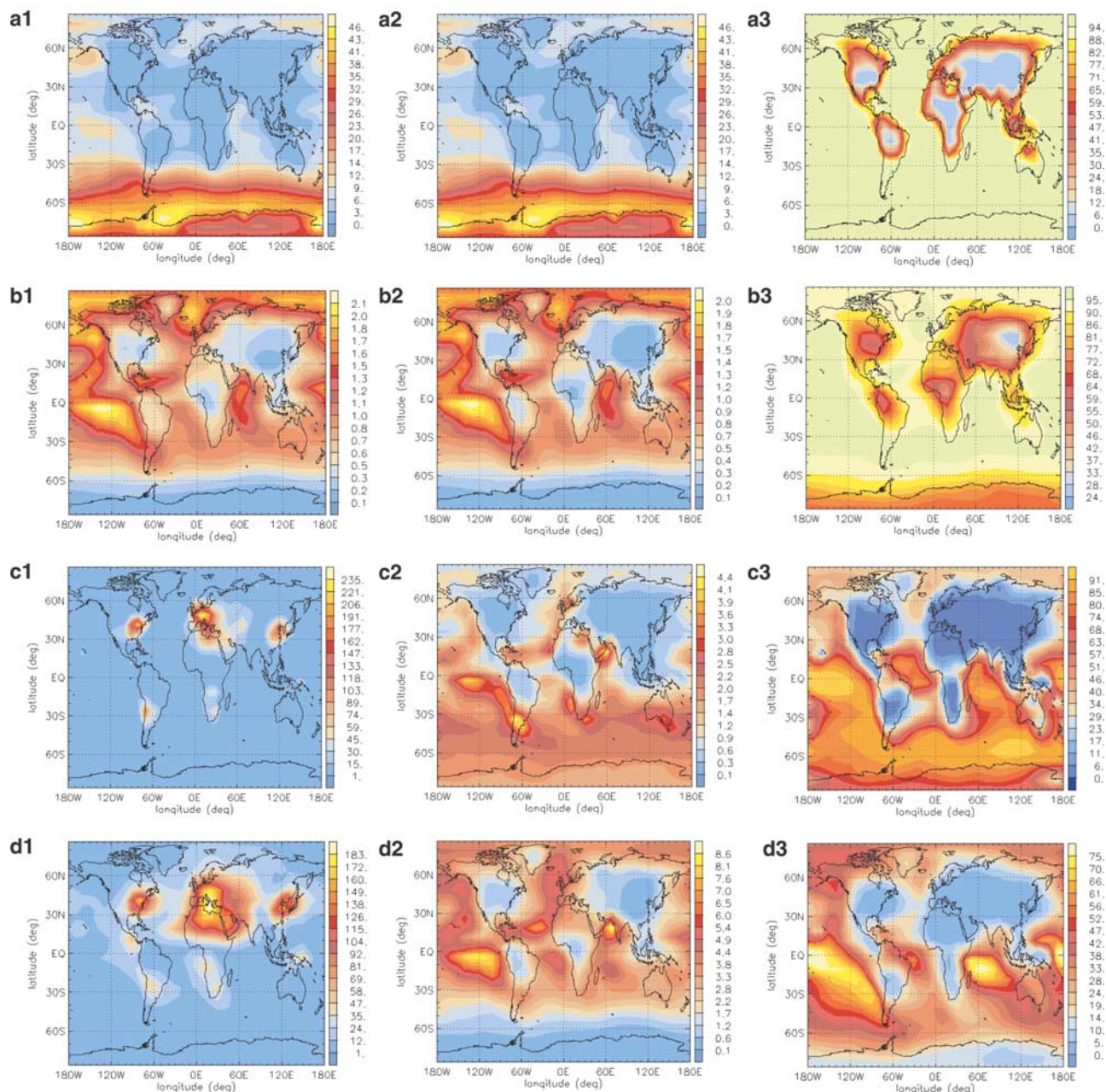
Figure 3.   Same as Figure 2, but for the months of June–July August.

3.2.   Methanesulphonate (MSA)

[27]   The spatial distribution of December–January–February and June–July August mean column burdens of MSA resulting from all sources are shown in plot b1 in Figures 2 and 3, respectively. The highest column burdens occur in summer (December–January–February in the Southern Hemisphere, up to 6.2 μmol m^{-2} and June–July August in the Northern Hemisphere, up to 2.1 μmol m^{-2}). These modeled patterns are consistent with observations by *Davison et al.* [1996]. While the TM3 model performs generally well in reproducing observed MSA measurements at most stations, it seems to consistently overpredict these concen-

trations above Greenland by approximately a factor of 10 (see Table 2). Comparisons with results from other model studies reveal TM3 simulation of the surface spatial distribution of MSA to be in close agreement with patterns simulated by *Koch et al.* [1999] and *Chin et al.* [2000a].

[28]   The MSA spatial distribution pattern during December–January–February reflects a drawing in of air from the Southern Ocean (where the highest concentrations occur) to the South Pacific, South Atlantic, and Indian Oceans by southeast trade winds. The highest concentrations occur to the east of the oceans, and become less toward the west as most of the aerosol is lost through deposition in its long-
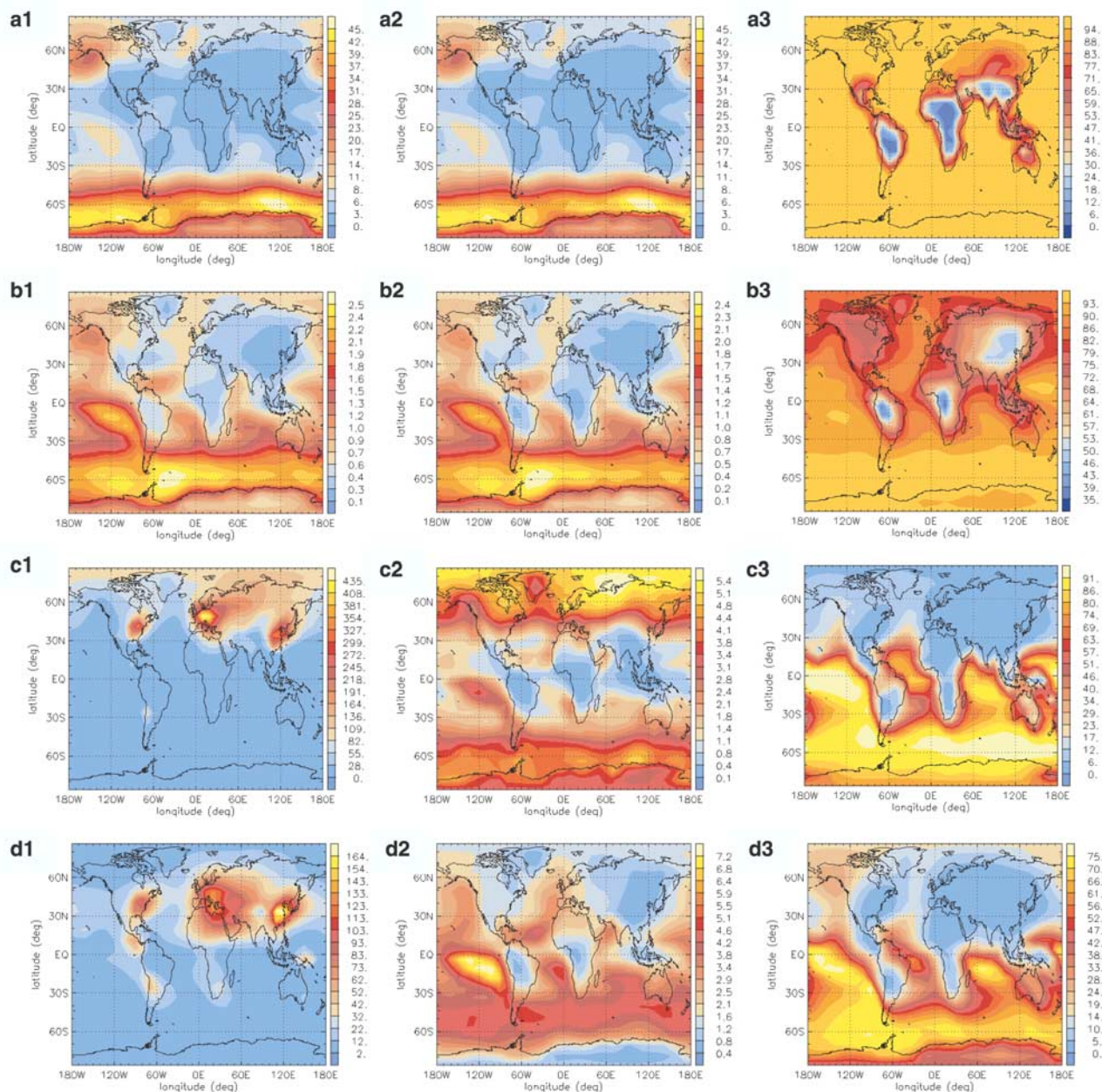
Figure 4. Same as Figure 2, but for an annually averaged period.

range transportation (Figure 2, plot b1). Air above these oceans has a descending motion, which suppresses precipitation and wet deposition. Removal of MSA is dominated by wet deposition [*Benkovitz et al.*, 1994] and so once this aerosol, and indeed nss SO$_4^=$ and soluble gases such as SO$_2$ (Figure 4, plots c2 and d2), are blown into these regions by trade winds, they are lost slowly and have a prolonged lifetime. At the annual scale, the highest annually averaged burdens of MSA resulting from all sources (up to 2.5 μmol m^{-2}) occur in the Southern Hemisphere, specifically above the Southern Ocean and South Pacific Ocean (plot b1 in Figures 5, 4, and 6). This is attributed to the high DMS burden in these regions (see Figure 4, plot a1). The high modeled burden of MSA above the Southern Ocean is in

agreement with long-term measurements made in the Southern Hemisphere (see Table 2).

[29] The global spatial distribution and magnitude of MSA column burdens resulting from DMS emissions of oceanic origin (plot b2 in Figures 2, 3, and 4, respectively) are largely identical to those of MSA resulting from all sources (also see plot b1 versus b2 in Figures 5 and 6). This is not surprising since atmospheric DMS oxidation is the only known source of MSA [*Huebert et al.*, 1993; *Legrand*, 1997; *Jefferson et al.*, 1998]. *Davison et al.* [1996] similarly found a coincidence of DMS and MSA concentration trends in shipboard measurements made along a transect through the Atlantic Ocean from the United Kingdom to Antarctica.
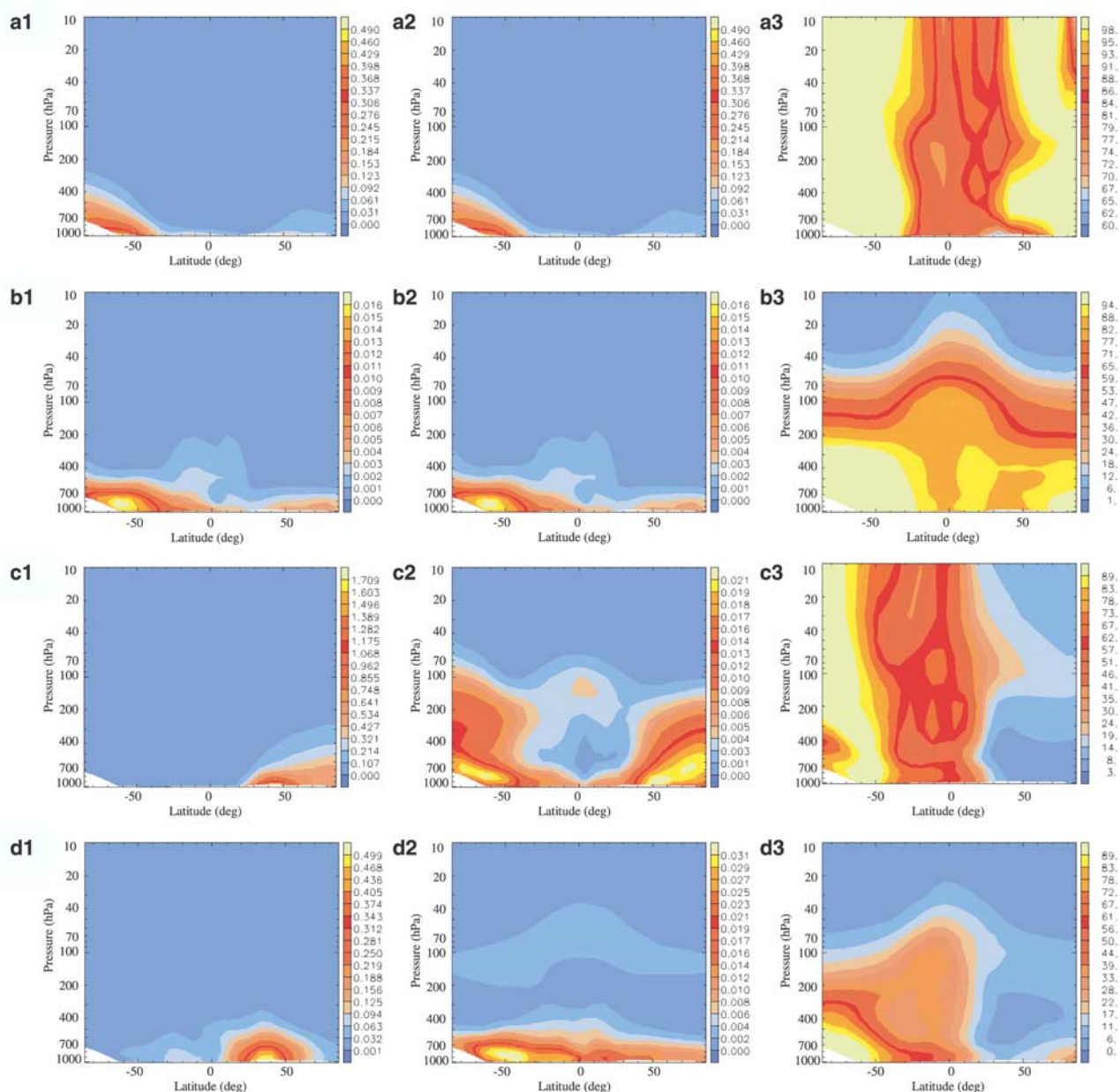
Figure 5. (a1, b1, c1, d1) Annual zonal mean vertical distributions (ppb) of DMS, MSA, SO$_2$ and nss SO$_4^=$, respectively, resulting from both oceanic and terrestrial sources; (a2, b2, c2, d2) those resulting from oceanic DMS emissions alone; and (a3, b3, c3, d3) the percentage of annually averaged zonal mean vertical distributions of DMS, MSA, SO$_2$ and nss SO$_4^=$, respectively, that can be attributed to oceanic DMS emissions alone.

[30] Differences in the DMS and MSA fields are noted around the polar regions (e.g., Figure 2, plot a1 versus b1 and plot a2 versus b2). In these examples, DMS exhibits an elevated burden around the Arctic region (where it is winter) while the MSA burden is elevated only in the Southern Hemisphere (where it is summer). This difference is caused by season- and light-induced variations in oxidant availability. In the dark winter period in the Northern Hemisphere, there is hardly any conversion of DMS to MSA since OH availability is light limited. As discussed earlier, MSA is produced only through the reaction of DMS

with the OH radical. The reaction of DMS with the nitrate radical produces only SO$_2$ as a product. Therefore, the DMS + NO$_3$ → SO$_2$ oxidation pathway is dominant in the dark winter months around polar regions. This is evident in Figure 2, plot c2, where SO$_2$ concentrations resulting from DMS oxidation are elevated around the Arctic region where DMS (but not MSA) burdens are also elevated.

[31] The globally averaged annual mean burden of MSA of oceanic origin is 0.95 μmol m^{-2} (94% of the total global MSA burden, Table 3). This huge contribution is not surprising since oceanic DMS emissions are globally the
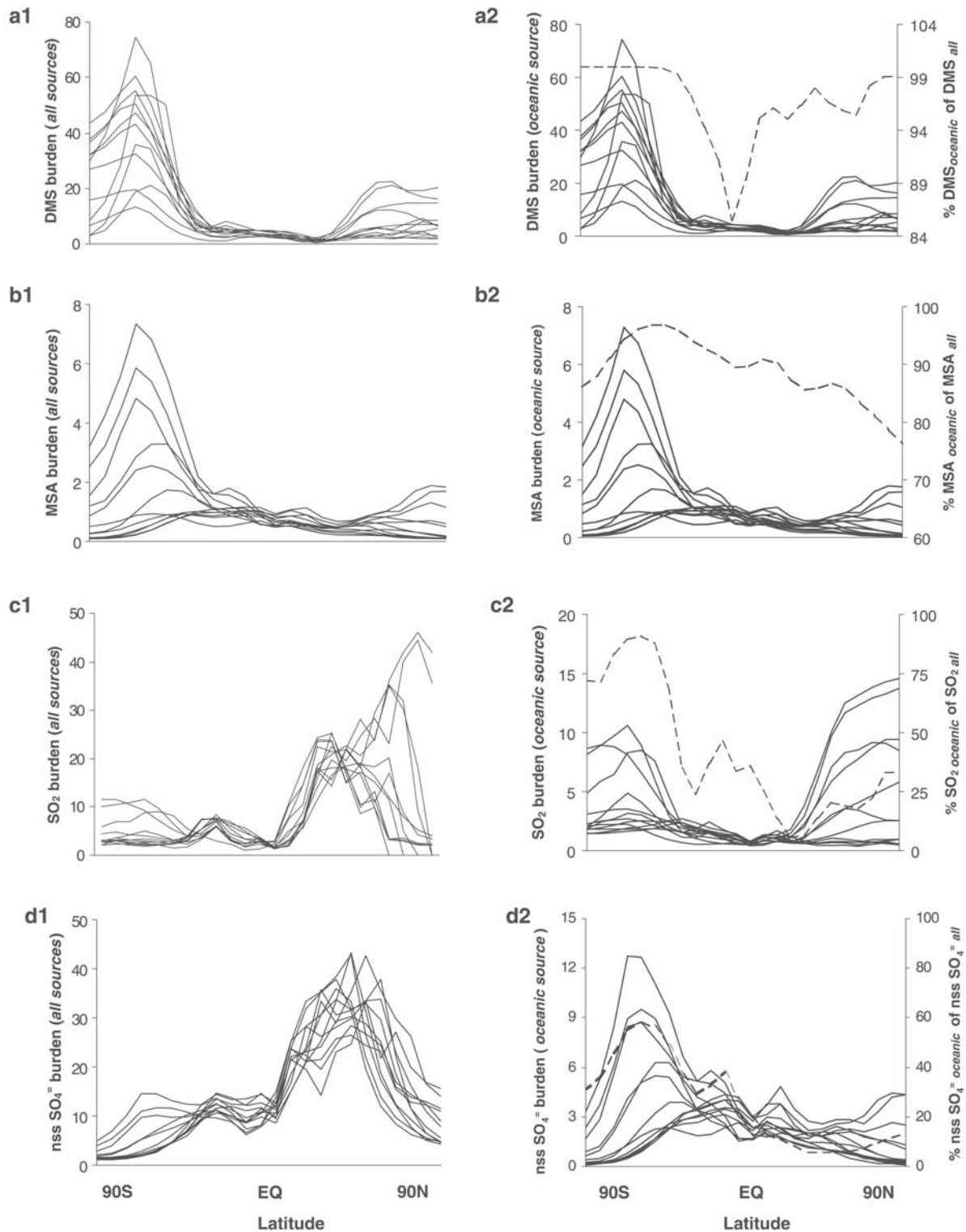
Figure 6. (a1, b1, c1, d1) Zonal monthly means of the atmospheric DMS, MSA, SO$_2$ and nss SO$_4^=$ column burdens respectively, resulting from both oceanic and terrestrial sources, and (a2, b2, c2, d2) those resulting from oceanic sources only. Dashed line in plots a2, b2, c2, and d2 shows the percentage of zonal annually averaged column burdens of DMS, MSA, SO$_2$ and nss SO$_4^=$, respectively, that can be attributed to oceanic DMS emissions alone.

Table 3. Mean Annual Column Burdens and Surface (1009 hPa/35 m) Concentrations of DMS, MSA, SO$_2$ and nss SO$_4^=$ Resulting From Both Oceanic and Terrestrial Sources ("Total") and From Oceanic DMS Emissions Alone ("Oceanic")[a]

	Annual Mean Column Burdens, µmol m^{-2}			Annual Mean Surface Concentrations, ppb		
	NH	SH	GLOBAL	NH	SH	GLOBAL
DMS oceanic	5.13	18.8	11.2	0.96	3.06	4.02
DMS total	5.24	18.9	12.1	1.02	3.12	4.14
% DMS oceanic of total	98	99	98	94	98	97
MSA oceanic	0.50	1.40	0.95	0.046	0.124	0.170
MSA total	0.56	1.45	1.01	0.049	0.125	0.174
% MSA oceanic of total	89	97	94	94	99	98
SO$_2$ oceanic	2.91	2.63	2.8	0.13	0.12	0.25
SO$_2$ total	13.3	4.3	8.8	8.02	0.39	8.41
% SO$_2$ oceanic of total	22	61	32	2	31	3
Nss SO$_4^=$ oceanic	1.8	3.2	2.5	0.15	0.26	0.41
Nss SO$_4^=$ total	20.9	7.4	14.2	2.66	0.48	3.14
% Nss SO$_4^=$ oceanic of total	9	43	18	6	54	13

[a]Percentage contribution of seawater DMS to the total burdens and surface concentrations are also presented.

largest MSA source. Plot b3 in Figures 2, 3, and 4 shows spatial distribution of the percentage of MSA that can be attributed to DMS emissions of oceanic origin. During December–January–February, the contribution of seawater DMS contributes to the total column burden of MSA is greatest in the Southern Hemisphere, where the atmospheric burden of its precursor DMS is also greatest. This contribution is lower over the Southern Hemispheric continental regions (where terrestrial sources are more important and oxidant levels are higher) and over the North Pole (where MSA advected from continental regions is also abundant). During June–July August and at the annual scale, the contribution of seawater DMS to the total column burden of MSA is greatest in all oceanic areas of the globe and lowest over continental regions (plot b3 in Figures 3 and 4).

3.3. Sulphur Dioxide (SO$_2$)

[32] The spatial distribution of SO$_2$ column burdens resulting from all sources (plot c1 in Figures 2, 3, and 4, respectively) reflect the overwhelming yearlong influence of anthropogenic sources in the Northern Hemisphere (also see Figure 5, plot c1). The highest burdens (up to 500 µmol m^{-2} in December–January–February; 150 µmol m^{-2} in June–July August; and 400 µmol m^{-2} mean annually) are noted around the major source regions of China, eastern Europe, and the eastern coast of the United States and the polar areas to their north.

[33] The global spatial distribution of SO$_2$ column burdens resulting from DMS emissions of oceanic origin (plot c2 in Figures 2, 3, and 4, respectively) differ from those resulting from all sources. During December–January–February and at the annual scale, the highest burdens occur in the midlatitude and polar regions of both hemispheres (also see plot c2 in Figures 5 and 6). The lowest burdens are noted within the tropics where the lifetime of SO$_2$ is short-

ened by relatively high concentrations of OH and H$_2$O$_2$ and convective transport to upper levels [*Roelofs et al.*, 1998]. During June–July August, high SO$_2$ burdens are noted above the oligotrophic areas of the global ocean, where high atmospheric pressure and suppressed precipitation prevail. Suppressed precipitation results in a lower removal rate of SO$_2$ through its aqueous phase conversion to sulphate by H$_2$O$_2$ and O$_3$.

[34] The globally averaged annual mean burden of SO$_2$ produced from oceanic DMS is 2.8 µmol m^{-2} (32% of the total global SO$_2$ burden). On a hemispheric scale, the contribution of seawater DMS to the mean annual column burden of SO$_2$ resulting from all sources is greatest in the Southern Hemisphere where it is estimated at 61% (Table 3, Figures 5 (plot c3), 4 (plot c3), and 6 (plot c2)). This contribution is less (22%) in the Northern Hemisphere where anthropogenic sources of SO$_2$ are dominant. During December–January–February and June–July August the contribution of seawater DMS to the total column burden of SO$_2$ is also greater in the Southern Hemisphere than in the Northern Hemisphere (plot c3 in Figures 2 and 3). Even though June–July August is winter in the Southern Hemisphere, elevated oceanic-derived SO$_2$ burdens occur over this area in this season due to a high DMS burden.

3.4. Non-Sea-Salt Sulphate (NSS SO$_4^=$)

[35] The spatial distribution of nss SO$_4^=$ column burdens resulting from all sources (plot d1 in Figures 2, 3, and 4, respectively) reflects the overwhelming yearlong influence of anthropogenic sources in the Northern Hemisphere (also see Figure 5, plot d1). This result is in agreement with long-term measurements of nss SO$_4^=$ from a network of monitoring stations spread across the North Atlantic ocean [*Prospero et al.*, 1995]. The highest burdens (up to 200 µmol m^{-2} in December–January–February; 180 µmol m^{-2} in June–July August; and 150 µmol m^{-2} mean annually) occur around the major source regions of China, eastern Europe, and the eastern coast of the United States. The spatial distribution pattern of nss SO$_4^=$ simulated by TM3 is in agreement with that simulated by *Koch et al.* [1999] and *Chin et al.* [2000a].

[36] The spatial distribution of the column burdens of nss SO$_4^=$ resulting from oceanic DMS (plot d2 in Figures 2, 3, and 4, respectively) differs from that of nss SO$_4^=$ resulting from all sources, but is similar to that of MSA aerosol, since both aerosols have common sinks and transport mechanisms. During December–January–February and at the annual scale, nss SO$_4^=$ is picked up from the Southern Ocean (where the highest concentrations occur, also see plot d2 in Figures 5 and 6) by southeast trade winds and is brought to the atmosphere above the South Pacific, South Atlantic, and Indian Oceans. Some interhemispheric transfer of this nss SO$_4^=$ is further evident and results in elevated concentrations in the tropical Northern Hemisphere. A consequence of this long range dispersion of this nss SO$_4^=$ is the spread of the climate-modulating effects of DMS to areas of low plankton activity and DMS production. During June–July August, elevated nss SO$_4^=$ burdens are noted above the oligotrophic areas of the global ocean, where high atmospheric pressure and suppressed precipitation prevail. Suppressed precipita-
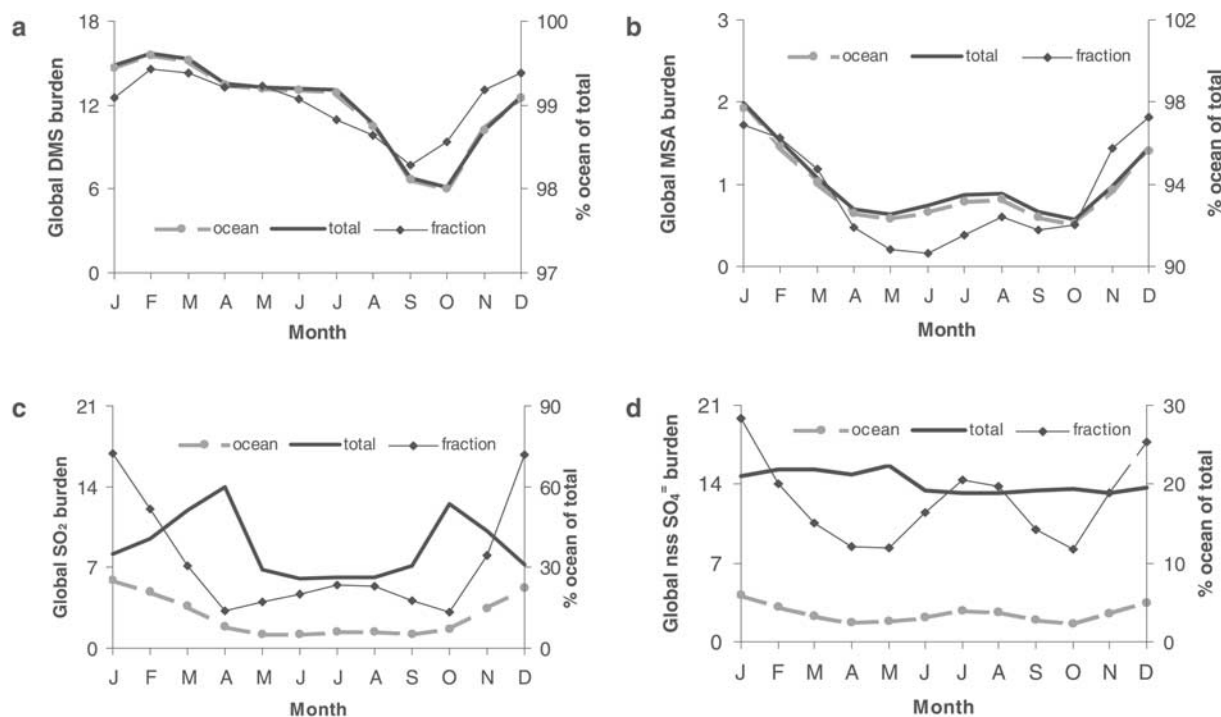
Figure 7. (a, b, c, d) Global monthly mean column burdens of DMS, MSA, SO$_2$ and nss SO$_4^=$, respectively. The global annual mean sulphur column burdens of oceanic algal origin are 12 μmol m^{-2} (99% of total global burden) for DMS; 1 μmol m^{-2} (94% of total global burden) for MSA; 2.8 μmol m^{-2} (32% of total global burden) for SO$_2$; and 2.5 μmol m^{-2} (18% of total global burden) for nss SO$_4^=$. The second y axis shows the percentage of the global monthly averaged sulphur column burden that can be attributed to oceanic DMS emissions alone.

tion results in reduced wet deposition, the main removal mechanism for SO$_4^=$ [*Langner and Rodhe*, 1991; *Huebert et al.*, 1993; *Benkovitz et al.*, 1994; *Lelieveld et al.*, 1997; *Chen et al.*, 2000].

[37] The globally averaged annual mean burden of nss SO$_4^=$ of oceanic algal origin is 2.5 μmol m^{-2} (18% of the total global nss SO$_4^=$ burden). On a hemispheric scale, the contribution of seawater DMS to the mean annual column burden of nss SO$_4^=$ is greatest in the Southern Hemisphere, where it is estimated at 43% (Table 3). This contribution is only 9% in the Northern Hemisphere (also see Figures 4 (plot d3) and 6 (plot d2)). During December–January–February and June–July August the contribution of seawater DMS to the total column burden of nss SO$_4^=$ is also greatest in the Southern Hemisphere (Figures 2 (plot d3) and 3 (plot d3)). Even though June–July August is winter in the Southern Hemisphere, elevated concentrations also occur over this area in this season due to a high burden of DMS (Figure 4, plot a1). The high modeled burden of nss SO$_4^=$ of oceanic DMS origin above the Southern Ocean is in agreement with long-term measurements made in the Southern Hemisphere [*Davison et al.*, 1996; *Ayers and Gillett*, 2000].

3.5. Combined Results (DMS, MSA, SO$_2$, and nss SO$_4^=$)

[38] The contribution of seawater DMS to annually averaged column burdens and surface concentrations (1009 hPa/35 m) of DMS, MSA, SO$_2$, and nss SO$_4^=$ is compared in Table 3. The spatial distribution of mean surface concentrations of DMS, MSA, SO$_2$, and nss SO$_4^=$ resulting from all sources and from oceanic sources only, largely resemble those exhibited by their column burdens during all periods and are consequently not presented here. We choose to present the burdens rather than the surface distributions as these are most relevant to climate considerations.

[39] Globally averaged monthly mean burdens of atmospheric DMS, MSA, SO$_2$, and nss SO$_4^=$ are presented in Figure 7. The temporal variability of the global mean of MSA closely follows that of its sole precursor atmospheric DMS, which in turn closely follows that of its major source seawater DMS. The highest global burdens of oceanic-derived DMS, MSA, SO$_2$, and nss SO$_4^=$ occur during the Southern Hemispheric summer months, when oceanic DMS emissions are greatest.

[40] The vertical distribution of annually averaged DMS, MSA, SO$_2$, and nss SO$_4^=$ concentrations resulting from all sources and from oceanic sources only shows maximum concentrations in the boundary layer followed by the free troposphere (Figure 5 and Table 1). These patterns are in agreement with vertical profile measurements over the Atlantic, Pacific, and Southern Oceans [e.g., *Ferek et al.*, 1986; *Luria et al.*, 1986, 1989; *Andreae et al.*, 1988, 1993; *Berresheim et al.*, 1990; *Johnson and Bates*, 1993; *Cooper and Saltzman*, 1993; *Li et al.*, 1993a; *Davison et al.*, 1996; *Koch et al.*, 1999; *Barth et al.*, 2000; *Chin et al.*, 2000b]. The highest concentrations resulting from all sources occur

at latitudes south of 50°S for DMS and MSA (where the atmospheric DMS burden is greatest) and at latitudes between 30°N and 60°N for SO_2 and nss SO_4^- (a region of overwhelmingly high industrial sulphur emissions; also see Table 1). Figure 5, plots a3 and c3, shows that the ratio of the gases DMS and SO_2 resulting from oceanic sources to those resulting from all sources is largely independent of elevation. MSA and nss SO_4^-, however, show a decrease in this ratio with elevation, due to scavenging by precipitation.

[41] While our study has improved upon several shortcomings in previous studies, the general accuracy of our model results is still constrained by a still-limited knowledge of DMS chemistry and kinetics; shortcomings in some TM3 parameterizations and percentage yields selected for DMS oxidation products under varying temperatures; possible underestimation of DMS fluxes by the Liss and Merlivat method of flux determination (as much as a factor 2) [*Bates et al.*, 1994; *Chin et al.*, 1996; *Turner et al.*, 1996; *Nightingale et al.*, 2000]; and the paucity of data points in the *Kettle et al.* [1999] DMS database and shortcomings in their data interpolation procedure. We have also not considered two possibly important products of DMS oxidation by OH: dimethylsulphoxide (DMSO) and dimethylsulphone (DMSO₂) [*Malin et al.*, 1992; *Lin and Chameides*, 1993; *Huebert et al.*, 1993; *Benkovitz et al.*, 1994; *Prospero et al.*, 1995; *Davis et al.*, 1998; *Jefferson et al.*, 1998; *Chen et al.*, 2000; *Arsene et al.*, 2001]. While progress is being made in understanding their chemistry and kinetics, areas of major uncertainty still exist and critical information that would strengthen model parameterizations is missing.

4. Conclusions

[42] Marine phytoplankton make an important contribution to the global sulphur cycle. Global three-dimensional chemical transport modeling shows that ocean-leaving DMS significantly contributes to the global annually averaged column burdens (from the surface to the lower stratosphere) of DMS (11.9 μmol m^{-2}, 98% of total global burden), MSA (0.95 μmol m^{-2}, 94% of total global burden), SO_2 (2.8 μmol m^{-2}, 32% of total global burden), and nss SO_4^- (2.5 μmol m^{-2}, 18% of total global burden). On a hemispheric scale, the contribution of seawater DMS to the mean annual column burden of nss SO_4^- (a climate-relevant aerosol) is greatest in the relatively pristine Southern Hemisphere, where it is estimated at 43%. This contribution is only 9% in the Northern Hemisphere, where anthropogenic sulphur sources are overwhelming. The huge contributions of oceanic DMS to the total atmospheric DMS and MSA burdens is not surprising since oceanic DMS emissions are globally the largest atmospheric DMS and MSA source. The global scope of our study has allowed identification of regions receiving the greatest marine algal-derived input of atmospheric sulphur components in the present-day climate scenario.

References

Albrecht, B. A., Aerosols, cloud microphysics, and fractional cloudiness, *Science*, *245*, 1227–1230, 1989.

Andreae, M. O., The ocean as a source of atmospheric sulphur compounds, in *The Role of Air-Sea Exchange in Geochemical Cycling*, edited by P. Buat-Menard, pp. 331–362, D. Reidel, Norwell, Mass., 1986.

Andreae, M. O., and P. J. Crutzen, Atmospheric aerosols: Biogeochemical sources and role in atmospheric chemistry, *Science*, *276*, 1052–1058, 1997.

Andreae, M. O., R. J. Ferek, F. Bermond, K. P. Byrd, R. T. Engstrom, S. Hardin, P. D. Houmere, F. LeMarrec, and H. Raemdonck, Dimethylsulphide in the marine atmosphere, *J. Geophys. Res.*, *90*, 12,891–12,900, 1985.

Andreae, M. O., H. Berresheim, T. W. Andreae, M. A. Kritz, T. S. Bates, and J. T. Merrill, Vertical distribution of dimethylsulphide, sulphur dioxide, aerosol ions and radon over the northeast Pacific Ocean, *Atmos. Chem.*, *6*, 149–173, 1988.

Andreae, T. W., M. O. Andreae, and H. G. Bingemer, Measurements of dimethylsulphide and H₂S over the western North Atlantic and the tropical Atlantic, *J. Geophys. Res.*, *98*, 23,389–23,396, 1993.

Andreae, T. W., M. O. Andreae, and G. Schebeske, Biogenic sulphur emissions and aerosols over the tropical South Atlantic: 1. Dimethylsulphide in seawater and in the atmospheric boundary layer, *J. Geophys. Res.*, *99*, 22,819–22,829, 1994.

Andreae, M. O., W. Elbert, and S. J. de Mora, Biogenic sulphur emissions and aerosols over the tropical south Atlantic: 3. Atmospheric dimethylsulphide, aerosols, and cloud condensation nuclei, *J. Geophys. Res.*, *100*, 11,335–11,356, 1995.

Andres, R. J., and A. D. Kasgnoc, A time-averaged inventory of subaerial volcanic sulphur emissions, *J. Geophys. Res.*, *103*, 25,251–25,261, 1998.

Arsene, C., I. Barnes, K. H. Becker, and R. Mocanu, FT-IR product study on the photo-oxidation of dimethylsulphide in the presence of NOₓ: Temperature dependence, *Atmos. Environ.*, *35*, 3769–3780, 2001.

Atkinson, R., Kinetics and mechanisms of the gas phase reactions of the NO₃ radical with organic compounds, *J. Phys. Chem. Ref. Data*, *20*, 459–507, 1991.

Atkinson, R., J. N. Pitts Jr., and S. M. Aschmann, Tropospheric reactions of dimethylsulphide with NO₃ and OH radicals, *J. Phys. Chem.*, *88*, 1584–1587, 1984.

Atkinson, R., D. L. Baulch, R. A. Cox, R. F. Hampson Jr., J. A. Kerr, and J. Troe, Evaluated kinetic and photochemical data for atmospheric chemistry: Supplement IV, *Atmos. Environ., Part A*, *26*, 1187–1230, 1992.

Atkinson, R., D. L. Baulch, R. A. Cox, R. F. Hampson Jr., J. A. Kerr, M. J. Rossi, and J. Troe, Evaluated kinetic and photochemical data for atmospheric chemistry: Supplement VI-IUPAC subcommittee on gas kinetic data evaluation for atmospheric chemistry, *J. Phys. Chem. Ref. Data*, *26*, 1329–1499, 1997.

Ayers, G. P., and R. W. Gillett, DMS and its oxidation products in the remote marine atmosphere: Implications for climate and atmospheric chemistry, *J. Sea Res.*, *43*, 275–286, 2000.

Ayers, G. P., J. P. Ivey, and H. S. Goodman, Sulphate and methanesulphonate in the maritime aerosol at Cape Grim, Tasmania, *J. Atmos. Chem.*, *4*, 173–185, 1986.

Ayers, G. P., J. P. Ivey, and R. W. Gillett, Coherence between seasonal cycles of dimethylsulphide, methanesulphonate and sulphate in marine air, *Nature*, *349*, 404–406, 1991.

Barone, S. B., A. A. Turnipseed, and A. R. Ravishankara, Role of adducts in the atmospheric oxidation of dimethylsulphide, *Faraday Discuss.*, *100*, 39–54, 1995.

Barth, M. C., P. J. Rasch, J. T. Kiehl, C. M. Benkovitz, and S. E. Schwartz, Sulphur chemistry in the National Center for Atmospheric Research Community Climate Model: Description, evaluation, features and sensitivity to aqueous chemistry, *J. Geophys. Res.*, *105*, 1387–1415, 2000.

Bates, T. S., and P. K. Quinn, Dimethylsulphide (DMS) in the equatorial Pacific Ocean (1982–1996): Evidence of a climate feedback?, *Geophys. Res. Lett.*, *24*, 861–864, 1997.

Bates, T. S., R. J. Charlson, and R. H. Gammon, Evidence for the climatic role of marine biogenic sulphur, *Nature*, *329*, 319–321, 1987.

Bates, T. S., B. K. Lamb, A. Guenther, J. Dignon, and R. E. Stoiber, Sulphur emissions to the atmosphere from natural sources, *J. Atmos. Chem.*, *14*, 315–337, 1992a.

Bates, T. S., J. A. Calhoun, and P. K. Quinn, Variations in the methane-sulfonate to sulfate molar ratio in sub-µm marine aerosol particles over the South Pacific Ocean, *J. Geophys. Res.*, *97*, 9859–9865, 1992b.

Bates, T. S., R. P. Kiene, G. V. Wolfe, P. A. Matrai, F. P. Chavez, K. R. Buck, R. W. Blomquist, and R. L. Cuhel, The cycling of sulfur in surface seawater of the northeast Pacific, *J. Geophys. Res.*, *99*, 7835–7843, 1994.

Benkovitz, C. M., C. M. Berkowitz, R. C. Easter, S. Nemesure, R. Wagener, and S. E. Schwartz, Sulphate over the North Atlantic and adjacent continental regions: Evaluation for October and November 1986 using a three-dimensional model driven by observation-derived meteorology, *J. Geophys. Res.*, *99*, 20,725–20,756, 1994.

Berresheim, H., Biogenic sulphur emissions from the Subantarctic and Antarctic Oceans, *J. Geophys. Res.*, *92*, 13,245–13,262, 1987.

Berresheim, H., M. O. Andreae, G. P. Ayers, R. W. Gillett, J. T. Merrill, V. J. Davis, and W. L. Chameides, Airborne measurements of dimethylsulphide, sulphur dioxide and aerosol ions over the Southern Ocean south of Australia, *J. Atmos. Chem.*, *10*, 341–370, 1990.

Berresheim, H., M. O. Andreae, R. L. Iverson, and S. M. Li, Seasonal variations of dimethylsulphide emissions and atmospheric sulphur and nitrogen species over the western North Atlantic Ocean, *Tellus, Ser. B*, *43*, 353–372, 1991.

Berresheim, H., J. W. Huey, R. P. Thorn, F. L. Eisele, D. J. Tanner, and A. Jefferson, Measurements of dimethylsulphide, dimethylsulphoxide, dimethylsulphone and aerosol ions at Palmer Station, Antarctica, *J. Geophys. Res.*, *103*, 1629–1637, 1998.

Boucher, O., and U. Lohmann, The Sulfate-CCN-Cloud albedo effect: A sensitivity study with two general circulation models, *Tellus, Ser. B*, *47*, 281–300, 1995.

Boucher, O., and M. Pham, History of sulphate aerosol radiative forcings, *Geophys. Res. Lett.*, *29*, 1308, 10.1029/2001GL014048, 2002.

Burgermeister, S., R. L. Zimmermann, H. W. Georgii, H. G. Bingemer, G. O. Kirst, M. Janssen, and W. Ernst, On the biogenic origin of dimethylsulphide: Relation between chlorophyll, ATP, organismic DMSP, phytoplankton species, and DMS distribution in Atlantic surface water and atmosphere, *J. Geophys. Res.*, *95*, 20,607–20,615, 1990.

Capaldo, K., J. J. Corbett, P. Kasibhatla, P. Fischbeck, and S. N. Pandis, Effects of ship emissions on sulphur cycling and radiative climate forcing over the ocean, *Nature*, *400*, 743–746, 1999.

Charlson, R. J., J. E. Lovelock, M. O. Andreae, and S. G. Warren, Oceanic plankton, atmospheric sulphur, cloud albedo and climate, *Nature*, *326*, 655–661, 1987.

Charlson, R. J., S. E. Schwartz, J. M. Hales, R. D. Cess, J. A. Coakley Jr., J. E. Hansen, and D. J. Hofmann, Climate forcing by anthropogenic aerosols, *Science*, *255*, 423–430, 1992.

Chen, G., D. D. Davis, P. Kasibhatla, A. R. Bandy, D. C. Thornton, B. J. Huebert, A. D. Clarke, and B. W. Blomquist, A study of DMS oxidation in the tropics: Comparison of Christmas Island field observation of DMS, SO$_2$, and DMSO with model simulations, *J. Atmos. Chem.*, *37*, 137–160, 2000.

Chin, M., and D. J. Jacob, Anthropogenic and natural contributions to tropospheric sulphate: A global model analysis, *J. Geophys. Res.*, *101*, 18,691–18,699, 1996.

Chin, M., D. J. Jacob, G. M. Gardner, M. S. Foreman-Fowler, P. A. Spiro, and D. L. Savoie, A global three-dimensional model of tropospheric sulphate, *J. Geophys. Res.*, *101*, 18,667–18,690, 1996.

Chin, M., R. B. Rood, S.-J. Lin, J.-F. Muller, and A. M. Thompson, Atmospheric sulphur cycle in the global model GOCART: Model description and global properties, *J. Geophys. Res.*, *105*, 24,671–24,687, 2000a.

Chin, M., D. L. Savoie, B. J. Huebert, A. R. Bandy, D. C. Thornton, T. S. Bates, P. K. Quinn, E. S. Saltzman, and W. J. De Bruyn, Atmospheric sulphur cycle simulated in the global model GOCART: Comparison with field observations and regional budgets, *J. Geophys. Res.*, *105*, 24,689–24,712, 2000b.

Cooper, D. J., and E. S. Saltzman, Measurements of Atmospheric dimethylsulphide, hydrogen sulphide and carbon disulphide during GTE/CITE 3, *J. Geophys. Res.*, *98*, 23,397–23,409, 1993.

Corbett, J. J., P. S. Fischbeck, and S. N. Pandis, Global nitrogen and sulphur inventories for ocean-going ships, *J. Geophys. Res.*, *104*, 3457–3470, 1999.

Crutzen, P. J., and P. H. Zimmermann, The changing photochemistry of the troposphere, *Tellus, Ser. A/B*, *43*, 136–151, 1991.

Dacey, J. W. H., and S. G. Wakeham, Oceanic dimethylsulphide: Production during zooplankton grazing on phytoplankton, *Science*, *233*, 1314–1316, 1986.

Davis, D., G. Chen, P. Kasibhatla, A. Jefferson, D. Tanner, F. Eisele, D. Lenschow, W. Neff, and H. Berresheim, DMS oxidation in the Antarctic marine boundary layer: Comparison of model simulations and field observations of DMS, DMSO, DMSO$_2$, H$_2$SO$_4$(g), MSA(g), and MSA(p), *J. Geophys. Res.*, *103*, 1657–1678, 1998.

Davison, B., and C. N. Hewitt, Natural sulphur species from the North Atlantic and their contribution to the United Kingdom sulphur budget, *J. Geophys. Res.*, *97*, 2475–2488, 1992.

Davison, B., C. O'Dowd, C. N. Hewitt, M. H. Smith, R. M. Harrison, D. A. Peel, E. Wolf, R. Mulvaney, M. Schwikowski, and U. Baltensperger, Dimethylsulphide and its oxidation products in the atmosphere of the Atlantic and Southern Oceans, *Atmos. Environ.*, *30*, 1895–1906, 1996.

De Bruyn, W. J., T. S. Bates, J. M. Cainey, and E. S. Saltzman, Shipboard measurements of dimethylsulphide and SO$_2$ southwest of Tasmania during the first Aerosol Characterisation Experiment (ACE 1), *J. Geophys. Res.*, *103*, 16,703–16,711, 1998.

Dentener, F., J. Feichter, and A. Jeuken, Simulation of the transport of Rn^{222} using on-line and off-line global models at different horizontal resolutions: A detailed comparison with measurements, *Tellus, Ser. B*, *51*, 573–602, 1999.

Dentener, F., J. Williams, and S. Metzger, Aqueous phase reaction of HNO$_4$: The impact on tropospheric chemistry, *J. Atmos. Chem.*, *41*, 109–134, 2002.

Feichter, J., and U. Lohmann, Can a relation technique be used to validate clouds and sulphur species in a GCM?, *Q.J.R. Meteorol. Soc.*, *125*, 1277–1294, 1999.

Feichter, J., E. Kjellström, H. Rodhe, F. Dentener, J. Lelieveld, and G. J. Roelofs, Simulation of tropospheric sulphur cycle in a global climate model, *Atmos. Environ.*, *30*, 1693–1707, 1996.

Feichter, J., U. Lohmann, and I. Schult, The atmospheric sulphur cycle in ECHAM-4 and its impact on the shortwave radiation, *Clim. Dyn.*, *13*, 235–246, 1997.

Ferek, R. J., R. B. Chatfield, and M. O. Andreae, Vertical distribution of dimethylsulphide in the marine atmosphere, *Nature*, *320*, 514–516, 1986.

Frost, T., and R. C. Upstill-Goddard, Air-sea gas exchange into the millenium: Progress and uncertainties, *Oceanogr. Mar. Biol.*, *37*, 1–45, 1999.

Gabric, A. J., G. Ayers, C. N. Murray, and J. Parslow, Use of remote sensing and mathematical modelling to predict the flux of dimethylsulphide to the atmosphere in the Southern Ocean, *Adv. Space Res.*, *18*(7), 117–128, 1996.

Gabric, A. J., P. H. Whetton, R. Boers, and G. P. Ayers, The impact of simulated climate change on the air-sea flux of dimethylsulphide in the subantarctic Southern Ocean, *Tellus, Ser. B*, *50*, 388–399, 1998.

Ghan, S. J., J. E. Penner, and K. E. Taylor, Sulphate aerosols and climate, *Nature*, *340*, 438, 1989.

Gillett, R. W., G. P. Ayers, J. P. Ivey, and J. L. Gras, Measurement of dimethylsulphide, sulphur dioxide, methane sulphonic acid and non sea salt sulphate at the Cape Grim baseline station, in *Dimethylsulphide: Oceans, Atmosphere and Climate*, edited by G. Restelli and G. Angeletti, pp 117–128, Kluwer Acad., Norwell, Mass., 1993.

Gondwe, M., W. Klaassen, W. Gieskes, and H. de Baar, Negligible direct radiative forcing of basin-scale climate by coccolithophore blooms, *Geophys. Res. Lett.*, *28*, 3911–3914, 2001.

Gregory, G. L., L. S. Warren, D. D. Davis, M. O. Andreae, A. R. Bandy, R. J. Ferek, J. E. Johnson, E. S. Saltzman, and D. J. Cooper, An intercomparison of instrumentation for tropospheric measurements of dimethylsulphide: Aircraft results for concentrations at the parts-per-trillion level, *J. Geophys. Res.*, *98*, 23,373–23,388, 1993.

Houweling, S., F. Dentener, and J. Lelieveld, The impact of nonmethane hydrocarbon compounds on tropospheric photochemistry, *J. Geophys. Res.*, *103*, 10,673–10,696, 1998.

Huebert, B. J., S. Howell, P. Laj, J. E. Johnston, T. S. Bates, P. K. Quinn, V. Yegorov, A. D. Clarke, and J. N. Porter, Observations of the atmospheric sulphur cycle on SAGA 3, *J. Geophys. Res.*, *98*, 16,985–16,995, 1993.

Hynes, A. J., P. H. Wine, and D. H. Semmes, Kinetics and mechanism of OH reactions with organic sulphides, *J. Phys. Chem*, *90*, 4148–4156, 1986.

Hynes, A. J., R. E. Stickel, A. J. Pounds, Z. Zhao, T. McKay, J. D. Bradshaw, and P. H. Wine, Mechanistic studies of the OH-initiated oxidation of dimethylsulphide, in *Dimethylsulphide: Oceans, Atmosphere and Climate*, edited by G. Restelli and G. Angeletti, pp. 211–221, Kluwer Acad., Norwell, Mass., 1993.

Jefferson, A., D. J. Tanner, F. L. Eisele, D. D. Davis, G. Chen, J. Crawford, J. W. Huey, A. L. Torres, and H. Berresheim, OH photochemistry and methane sulphonic acid formation in the coastal Antarctic boundary layer, *J. Geophys. Res.*, *103*, 1647–1656, 1998.

Jeuken, A. B. M., H. J. Eskes, P. F. J. van Velthoven, H. M. Kelder, and E. V. Holm, Assimilation of total ozone satellite measurements in a three-dimensional tracer transport model, *J. Geophys. Res.*, *104*, 5551–5563, 1999.

Jeuken, A., J. P. Veefkind, F. Dentener, S. Metzger, and C. Robles Gonzalez, Simulation of the aerosol optical depth over Europe for August 1997 and a comparison with observations, *J. Geophys. Res.*, *106*, 28,295–28,311, 2001.

Johnson, J. E., and T. S. Bates, Atmospheric measurements of carbonylsulphide, dimethylsulphide and carbondisulphide using the Electron Capture Sulphur Detector, *J. Geophys. Res.*, *98*, 23,411–23,421, 1993.

Kasibhatla, P., W. L. Chameides, and J. St. John, A three-dimensional global model investigation of seasonal variations in the atmospheric burden of anthropogenic sulphate aerosols, *J. Geophys. Res.*, *102*, 3737–3759, 1997.

Kettle, A. J., et al., A global database of sea surface dimethylsulphide (DMS) measurements and a procedure to predict sea surface DMS as a function of latitude, longitude and month, *Global Biogeochem. Cycles*, *13*, 399–444, 1999.

Kiene, R. P., and T. S. Bates, Biological removal of dimethylsulphide from sea water, *Nature*, *345*, 702–705, 1990.

Kiene, R. P., L. J. Linn, and J. A. Bruton, New important roles for DMSP in marine microbial communities, *J. Sea Res.*, *43*, 209–224, 2000.

Kirst, G. O., Osmotic adjustment in phytoplankton and macroalgae: The use of dimethylsulphoniopropionate (DMSP), in *Biological and Environmental Chemistry of DMSP and related Sulphonium Compounds*, edited by R. P. Kiene et al., pp. 121–129, Plenum, New York, 1996.

Koch, D., D. Jacob, I. Tegen, D. Rund, and M. Chin, Tropospheric sulphur simulation and sulphate direct radiative forcing in the Goddard Institute for Space Studies general circulation model, *J. Geophys. Res.*, *104*, 23,799–23,822, 1999.

Koga, S., and H. Tanaka, Numerical study of the oxidation process of dimethylsulphide in the marine atmosphere, *J. Atmos. Chem.*, *17*, 201–228, 1993.

Kouvarakis, G., and N. Mihalopoulos, Seasonal variation of dimethylsulphide in the gas phase and of methanesulphonate and non-sea-salt sulphate in the aerosols phase in the Eastern Mediterranean atmosphere, *Atmos. Environ.*, *36*, 929–938, 2002.

Kreidenweis, S. M., and J. H. Seinfeld, Nucleation of sulphuric acid-water and methanesulphonic acid-water solution particles: Implications for the atmospheric chemistry of organosulphur species, *Atmos. Environ.*, *22*, 283–296, 1988.

Kreidenweis, S. M., J. E. Penner, F. Yin, and J. H. Seinfeld, The effects of dimethylsulphide upon marine aerosol concentrations, *Atmos. Environ., Part A*, *25*, 2501–2511, 1991.

Langner, J., and J. Rodhe, A global three-dimensional model of the tropospheric sulphur cycle, *J. Atmos. Chem.*, *13*, 225–263, 1991.

Legrand, M., Ice-core records of atmospheric sulphur, *Philos. Trans. R. Soc. London, Ser. B*, *352*, 241–250, 1997.

Legrand, M., C. Feniet-Saigne, E. S. Saltzman, C. Germain, N. I. Barkov, and V. N. Petrov, Ice-core record of oceanic emissions of dimethylsulphide during the last climate cycle, *Nature*, *350*, 144–146, 1991.

Legrand, M., C. Hammer, M. De Angelis, J. Savarino, D. Delmas, H. Clausen, and S. J. Johnsen, Sulphur-containing species (methanesulphonate and SO_4) over the last climatic cycle in the Greenland Ice Core Project (central Greenland) ice core, *J. Geophys. Res.*, *102*, 26,663–26,679, 1997.

Lelieveld, J., G. J. Roelofs, L. Ganzeveld, J. Feichter, and H. Rodhe, Terrestrial sources and distribution of atmospheric sulphur, *Philos. Trans. R. Soc. London, Ser. B.*, *352*, 149–158, 1997.

Li, S. M., and L. A. Barrie, Biogenic sulphur aerosol in the Arctic troposphere: 1. Contributions to total sulphate, *J. Geophys. Res.*, *98*, 20,613–20,622, 1993.

Li, S. M., L. A. Barrie, R. W. Talbot, R. C. Harriss, C. I. Davidson, and J. L. Jaffrezo, Seasonal and geographic variations of methanesulphonic acid in the Arctic troposphere, *Atmos. Environ.*, *27*, 3011–3024, 1993a.

Li, S. M., L. A. Barrie, and A. Sirios, Biogenic sulphur aerosol in the Arctic troposphere: 2. Trends and seasonal variations, *J. Geophys. Res.*, *98*, 20,623–20,631, 1993b.

Lin, X., and W. L. Chameides, CCN formation from DMS without SO_2 acting as an intermediate, *Geophys. Res. Lett.*, *20*, 579–582, 1993.

Liss, P. S., and L. Merlivat, Air-sea gas exchange rates: Introduction and synthesis, in *The Role of Air-Sea Exchange in Geochemical Cycling*, edited by P. Buat-Menard, pp. 113–127, D. Reidel, Norwell, Mass., 1986.

Luria, M., C. C. Van Valin, D. L. Wellman, and R. F. Pueschel, Contribution of Gulf area natural sulphur to the North American sulphur budget, *Environ. Sci. Technol.*, *20*, 91–95, 1986.

Luria, M., C. C. Van Valin, J. N. Galloway, W. C. Keene, D. L. Wellman, H. Sievering, and J. F. Boatman, The relationship between dimethylsulphide and particulate sulphate in the mid-Atlantic ocean atmosphere, *Atmos. Environ.*, *23*, 139–147, 1989.

Malin, G., and G. O. Kirst, Algal production of dimethylsulphide and its atmospheric role, *J. Phycol.*, *33*, 889–896, 1997.

Malin, G., S. M. Turner, and P. S. Liss, Sulphur: The plankton/climate connection, *J. Phycol.*, *28*, 590–597, 1992.

Mulvaney, R., E. C. Pasteur, D. A. Peel, E. S. Saltzman, and P.-Y. Whung, The ratio of MSA to non-sea-salt sulphate in Antarctic Peninsula ice cores, *Tellus, Ser. B*, *44*, 295–303, 1992.

Nguyen, B. C., N. Mihalopoulos, J. P. Putaud, A. Gaudry, L. Gallet, W. C. Keene, and J. N. Galloway, Covariations in oceanic dimethylsulphide, its oxidation products and rain acidity at Amsterdam Island in the Southern Indian Ocean, *J. Atmos. Chem.*, *15*, 39–53, 1992.

Nightingale, P. D., G. Malin, C. S. Law, A. J. Watson, P. S. Liss, M. I. Liddicoat, J. Boutin, and R. C. Upstill-Goddard, In situ evaluation of air-sea gas exchange parameterisations using novel conservative and volatile tracers, *Global Biogeochem. Cycles*, *14*, 373–387, 2000.

O'Dowd, C. D., J. A. Lowe, M. H. Smith, B. Davison, C. N. Hewitt, and R. M. Harrison, Biogenic sulphur emissions and inferred non-sea-salt-sulphate cloud condensation nuclei in and around Antarctica, *J. Geophys. Res.*, *102*, 12,839–12,854, 1997.

Olivier, J. G. J., and J. J. M. Berdowski, Global emission sources and sinks, in *The Climate System*, edited by J. Berdowski et al., pp. 33–77, Swets and Zeitlinger, Lisse, Netherlands, 2001.

Penkett, S. A., B. M. R. Jones, K. A. Brice, and A. E. J. Eggleton, The importance of atmospheric ozone and hydrogen peroxide in oxidising sulphur dioxide in cloud and rainwater, *Atmos. Environ.*, *13*, 123–137, 1979.

Pham, M., J.-F. Muller, G. P. Brasseur, C. Granier, and G. Megie, A 3D model study of the global sulphur cycle: Contributions of anthropogenic and biogenic sources, *Atmos. Environ.*, *10–11*, 1815–1822, 1996.

Prospero, J. M., D. L. Savoie, E. S. Saltzman, and R. Larsen, Impact of oceanic sources of biogenic sulphur on sulphate aerosol concentrations at Mawson, Antarctica, *Nature*, *350*, 221–223, 1991.

Prospero, J. M., D. L. Savoie, R. Arimoto, H. Olafsson, and H. Hjartarson, Sources of aerosol nitrate and non-sea-salt sulphate in the Iceland region, *Sci. Total Environ.*, *160/161*, 181–191, 1995.

Quinn, P. K., S. F. Marshall, T. S. Bates, D. S. Covert, and V. N. Kapustin, Comparison of measured and calculated aerosol properties relevant to the direct radiative forcing of tropospheric sulfate aerosol on climate, *J. Geophys. Res.*, *100*, 8977–8991, 1995.

Raes, F., R. van Dingenen, E. Vignati, J. Wilson, J. P. Putaud, J. H. Seinfeld, and P. Adams, Formation and cycling of aerosols in the global troposphere, *Atmos. Environ.*, *34*, 4215–4240, 2000.

Rasch, P. J., M. C. Barth, J. T. Kiehl, S. E. Schwartz, and C. M. Benkovitz, A description of the global sulphur cycle and its controlling processes in the National Center for Atmospheric Research Community Climate Model, Version 3, *J. Geophys. Res.*, *105*, 1367–1385, 2000.

Roelofs, G. J., J. Lelieveld, and L. Ganzeveld, Simulation of global sulphate distribution and the influence on effective cloud drop radii with a coupled photochemistry-sulphur cycle model, *Tellus, Ser. B*, *50*, 224–242, 1998.

Saltzman, E. S., and D. J. Cooper, Shipboard measurements of atmospheric dimethylsulphide and hydrogen sulphide in the Caribbean and Gulf of Mexico, *J. Atmos. Chem.*, *7*, 191–209, 1988.

Saltzman, E. S., D. L. Savoie, R. G. Zika, and J. M. Prospero, Methane sulfonic acid in the marine atmosphere, *J. Geophys. Res.*, *88*, 10,897–10,902, 1983.

Saltzman, E. S., D. L. Savoie, J. M. Prospero, and R. G. Zika, Atmospheric methanesulphonic acid and non-sea salt sulphate at Fanning and American Samoa, *Geophys. Res. Lett.*, *12*, 437–440, 1985.

Savoie, D. L., and J. M. Prospero, Comparison of oceanic and continental sources of non-sea salt sulphate over the Pacific Ocean, *Nature*, *339*, 685–687, 1989.

Savoie, D. L., J. M. Prospero, and E. S. Saltzman, Nitrate, non-sea-salt sulphate and methanesulphonate over the Pacific ocean, in *Chemical Oceanography*, vol. 10, edited by J. P. Riley et al., pp. 219–250, Academic, San Diego, Calif., 1989.

Savoie, D. L., J. M. Prospero, R. J. Larsen, and E. S. Saltzman, Nitrogen and sulphur species in aerosols at Mawson, Antarctica, and their relationship to natural radionuclides, *J. Atmos. Chem.*, *14*, 181–204, 1992.

Savoie, D. L., J. M. Prospero, R. J. Larsen, F. Huang, M. A. Izaguirre, T. Huang, T. H. Snowdon, L. Custals, and C. G. Sanderson, Nitrogen and sulphur species in Antarctic Aerosols at Mawson, Palmer Station, and Marsh (King George Island), *J. Atmos. Chem.*, *17*, 95–122, 1993.

Savoie, D. L., J. M. Prospero, R. Arimoto, and R. A. Duce, Non-sea-salt sulphate and methanesulphonate at American Samoa, *J. Geophys. Res.*, *99*, 3587–3596, 1994.

Schwartz, S. E., Are global cloud albedo and climate controlled by marine phytoplankton?, *Nature*, *336*, 441–445, 1988.

Sciare, J., E. Baboukas, M. Kanakidou, U. Krischke, S. Belviso, H. Bardouki, and N. Mihalopoulos, Spatial and temporal variability of atmospheric sulphur-containing gases and particles during the Albatross campaign, *J. Geophys. Res.*, *105*, 14,433–14,448, 2000.

Spiro, P. A., D. J. Jacob, and J. A. Logan, Global inventory of sulphur emissions with 1° × 1° resolution, *J. Geophys. Res.*, *97*, 6023–6036, 1992.

Staubes, R., and H. W. Georgii, Biogenic sulphur compounds in seawater and the atmosphere of the Antarctic region, *Tellus, Ser. B*, *45*, 127–137, 1993.

Stefels, J., Physiological aspects of the production and conversion of DMSP in marine algae and higher plants, *J. Sea Res.*, *43*, 183–197, 2000.

Steil, B., M. Dameris, C. Bruhl, P. J. Crutzen, V. Grewe, M. Ponater, and R. Sausen, Development of a chemistry module for GCMs: First results of a multiannual integration, *Ann. Geophys.*, *16*, 205–228, 1998.

Suhre, K., M. O. Andreae, and R. Rosset, Biogenic sulphur emissions and aerosols over the tropical South Atlantic: 2. One-dimensional simulation of sulphur chemistry in the marine boundary layer, *J. Geophys. Res.*, *100*, 11,323–11,334, 1995.

Sunda, W., D. J. Kieber, R. P. Kiene, and S. Huntsman, An antioxidant function for DMSP and DMS in marine algae, *Nature*, *418*, 317–320, 2002.

Thompson, A. M., et al., Ozone observations and a model of marine boundary layer photochemistry during SAGA 3, *J. Geophys. Res.*, *98*, 16,955–16,968, 1993.

Turner, S. M., G. Malin, P. D. Nightingale, and P. S. Liss, Seasonal variation of dimethylsulphide in the North Sea and an assessment of fluxes to the atmosphere, *Mar. Chem.*, *54*, 245–262, 1996.

Tyrell, T., P. M. Holligan, and C. D. Mobley, Optical impacts of oceanic coccolithophore blooms, *J. Geophys. Res.*, *104*, 3223–3241, 1999.

Watson, A. J., R. C. Upstill-Goddard, and P. S. Liss, Air-Sea exchange in rough and stormy seas measured by a dual-tracer technique, *Nature*, *349*, 145–147, 1991.

Wayne, R. P., et al., The nitrate radical: Physics, chemistry and the atmosphere, *Atmos. Environ., Part A*, *25*, 1–203, 1991.

Wylie, D. J., and S. J. de Mora, Atmospheric dimethylsulphide and sulphur species in aerosol and rainwater at a coastal site in New Zealand, *J. Geophys. Res.*, *101*, 21,041–21,049, 1996.

———————————

H. de Baar, W. Gieskes, M. Gondwe, and W. Klaassen, Marine Biology Department, University of Groningen, Kerklaan 30, 9751 NN Haren, Netherlands. (debar@nioz.nl; w.w.c.gieskes@boil.rug.nl; p.m.van.himbergen@biol.rug.nl; w.klaassen@boil.rug.nl)

M. Krol, Institute for Marine and Atmospheric Research (IMAU), University of Utrecht, Princetonplein 5, 3584 CC Utrecht, Netherlands. (m.krol@phys.uu.nl)